Programmed knock-out of the *omega-1* gene of the blood fluke *Schistosoma mansoni*

Wannaporn Ittiprasert[1], Victoria H. Mann[1], Shannon E. Karinshak[1], Apisit Chaidee[1,2], Toshihiko Tanno[3], Chutima Kumkhaek[4], Pannathee Prangtaworn[1,5], Margaret Mentink-Kane[6], Geetha Sankaranarayan[7], Avril Coghlan[7], Christina J. Cochran[1], Gabriel Rinaldi[7], Patrick Driguez[7], Nancy Holroyd[7] Alan Tracey[7], Rutchanee Rodpai[1,2], Bart Everts[8], Cornelis H. Hokke[8], Karl F. Hoffmann[9], Matthew Berriman[7], Paul J. Brindley[1,*]

1. Department of Microbiology, Immunology & Tropical Medicine, & Research Center for Neglected Diseases of Poverty, School of Medicine & Health Sciences, George Washington University, Washington, D.C. 20037, USA

2. Department of Parasitology, Faculty of Medicine, Khon Kaen University, Khon Kaen, 40002, Thailand

3. Department of Surgery and the Institute of Human Virology, University of Maryland, Baltimore, MD 21201, USA

4. Cellular and Molecular Therapeutics Laboratory, National Heart, Lungs and Blood Institute, National Institutes of Health, Bethesda, MD 20814 USA

5. Department of Parasitology, Faculty of Medicine Siriraj Hospital, Mahidol University, Bangkok, Thailand 10700

6. Schistosomiasis Resource Center, Biomedical Research Institute, Rockville, MD 20850, USA

7. Wellcome Sanger Institute, Wellcome Genome Campus, Hinxton, CB10 1SA, UK

8. Department of Parasitology, Leiden University Medical Center, Leiden, Netherlands

9. Institute of Biological, Environmental & Rural Sciences (IBERS), Aberystwyth University, Aberystwyth, SY23 3DA, UK

Running title **Genome editing of schistosome *omega-1***

Keywords: *Schistosoma mansoni*; genome editing; Cas9; omega1; ribonuclease; flatworms; Platyhelminthes; functional genomics; lentivirus; homology directed repair; non-homologous end joining; double stranded break; Th2 phenotype; monocytic macrophage cell; granuloma;

[*]Correspondence, Paul Brindley, pbrindley@gwu.edu

Abstract

Soluble egg antigen (SEA) and excretory-secretory (ES) products of the egg of *Schistosoma mansoni* contain a glycosylated T2 family ribonuclease termed omega-1 (ω1). Following release from the egg, ω1 instructs antigen presenting cells to induce naïve $CD4^+$ T cells to mature into T helper 2 effectors that, in turn, establish the Th2 immunological phenotype characteristic of schistosomiasis. Here, schistosome eggs were either transiently exposed to recombinant Cas9 complexed with a synthetic guide RNA (sgRNA) of 20 nt complementary to exon 1 of ω1 by electroporation or transduced with pseudotyped lentivirus encoding Cas9 and this sgRNA. Subsequently, some eggs also were transduced with a single stranded oligodeoxynucleotide donor transgene that coded for a stop codon in all six frames, flanked by 50 nt-long 5'- and 3'-homology arms matching the predicted Cas9-catalyzed double stranded break (DSB) within *ω1*. CRISPResso analysis of amplicons spanning the predicted DSB revealed ~4.5% of the reads (total reads $>2\times10^6$ per treated sample) were mutated by insertions, deletions and/or substitutions, with an efficiency for homology directed repair of 0.19% insertion of the donor transgene. Messenger RNAs encoding *ω1* were reduced >80%, and soluble egg antigen (SEA) from ω1-mutated eggs exhibited markedly reduced ribonuclease activity, indicative that programmed Cas9 cleavage mutated the *ω1* gene. Following injection of schistosome eggs into the tail vein of BALB/c mice, the volume of pulmonary granulomas surrounding wild type eggs was 18-fold greater than ω1-mutated eggs, $6.21\times10^{-2} \pm 1.61\times10^{-3}$ versus $0.34\times10^{-2} \pm 0.12\times10^{-4}$ mm^3, respectively. In parallel, whereas wild-type SEA polarized Th2 cytokine responses including IL-4 and IL-5 in human monocyte/T cell co-cultures, significantly reduced levels of these cytokines followed the exposure to ω1-mutated SEA. In overview, programmed genome editing was active in schistosomes, Cas9-catalyzed chromosomal breakage was repaired by homology directed repair and/or non-homologous end-joining, and mutation of ω1 impeded the capacity of schistosome eggs to drive Th2 polarization and to provoke formation of pulmonary circumoval granulomas. These findings demonstrated for the first time the utility of CRISPR/Cas9-based genome editing for functional genomics for schistosomes.

Introduction

Schistosomiasis is considered the most problematic of the human helminth diseases in terms of morbidity and mortality [1-4]. The past decade has seen major advances in knowledge and understanding of the pathophysiology, developmental biology, evolutionary relationships and genome annotation of the human schistosomes [5-16]. As with other diseases, adapting CRISPR/Cas9 genome editing for functional genomics of schistosomes will drive innovation to enable deeper knowledge of schistosome pathogenesis, biology and evolution [17], and provide stable site-specific gene mutation and phenotype in contrast to retroviral transgene based RNA interference [16]. The schistosome egg plays a central role both in the transmission of the disease and in pathogenesis [1]. The appearance of *S. mansoni* eggs by six to eight weeks following infection coincides with profound polarization to a granulomatous, T helper 2 (Th2) phenotype [18-22]. Several egg proteins have been characterized, with >1,000 identified in soluble extracts (SEA, soluble egg antigen) [23-26]. In the viable egg, about 30 of these soluble proteins are located outside the developing miracidium and encompass the complement of secreted antigens (egg-secreted proteins, ESP) that interact with host tissues to facilitate passage of the egg from the mesenteric veins to the lumen of the intestines [27].

The T2 ribonuclease ω1 (omega-1) is the principal Th2-inducing component of ESP with Th2-polarizing activity requiring both RNase activity and ω1 glycosylation [19, 20, 28]. This RNase is hepatotoxic [29], secreted by the egg into the granuloma, and regulates the pattern recognition receptor signaling pathways in dendritic cells that, in turn, prime Th2 responses from $CD4^+$ cells [30]. Secreted ω1 provokes granulomatous inflammation around eggs traversing the wall of the intestines, and trapped in hepatic sinusoids and elsewhere, driving fibrosis that eventually results as hepatointestinal schistosomiasis [1, 31]. Here, we investigated the feasibility of programmed genome editing using CRISPR/Cas9 [32, 33] in schistosomes, aiming to edit the *ω1* locus for both gene knockout and knock-in. The investigation revealed that programmable genome editing catalyzed by the bacterial endonuclease Cas9 was active in schistosomes, with chromosomal double stranded breaks (DSB) repaired by homologous recombination directed repair (HDR) using a donor, single stranded oligonucleotide template bearing short homology arms and/or by non-homologous end joining (NHEJ). The programmed mutagenesis decreased levels of ω1 mRNA and induced distinct *in vitro* and *in vivo* phenotypes, including a substantial loss of capacity of SEA from ω1-mutated eggs to polarize Th2 cytokine responses (IL-4 and IL-5) in co-cultured dendritic and T cells and loss of capacity to provoke formation of pulmonary granulomas in BALB/c mice. The findings highlighted the utility of programmed genome editing for functional genomics for schistosomes.

Results

Omega-1, a multicopy locus on chromosome 1 of *S. mansoni*

Five genomic copies of *ω1* (*omega-1*) on chromosome 1 were identified in the genome of *S. mansoni*, versions 5 and 7 (Fig. S1) [12]. A single copy of *ω1* selected for genome editing includes four exons separated by three introns and spans 2,569 nt (Smp_193860, Uniprot Q2Y2H0_SCHMA) (Fig. 1A). Other copies have discrete exon/intron structure (that may partly reflect imprecise annotation) (Fig. S1) although the predicted amino acid sequences of copies are highly conserved. The predicted open reading frame (ORF) of Smp_193860 encodes a T2 ribonuclease of ~15 kDa, which lacks 5′ exons coding for a conserved amino acids region 1 (CASI) catalytic region, although it does include the CASII, and is smaller than the 31 kDa reported for ω1 [34]. The sgRNA targeted residues 164 to 183 of the predicted exon 1 of Smp_193860 adjacent to the protospacer adjacent motif (PAM), AGG, with the predicted Cas9 cleavage site located at three residues upstream of this PAM. The AGG and the nucleotide sequence complementary to this sgRNA were present on two of the other copies of *ω1*, Smp_179960 and Smp_184360, which shared >99% identity to Smp_193860. The coding sequences of the gene copies of *ω1* differed by several substitutions (Fig. S2, panels A-D).

NHEJ pathway genes in schistosomes

Artemis and DNA-PKcs are essential NHEJ factors in vertebrates [35, 36]. By searching for *S. mansoni* genes with the same Pfam domain content known for human NHEJ pathway genes, candidates for homologues six of seven human NHEJ pathway genes in *S. mansoni* were identified (Table S1) although a putative homologue of Cernunnos/XLF was not apparent in the genome of *S. mansoni* [36]. The human Cernunnos/XLF gene includes the Pfam XLF domain (PF09302), but this domain appears to be absent from genes in any flatworm species using the dataset of the International Helminth Genomes Consortium [37].

Site-specific integration of exogenous DNA confirmed CRISPR-Cas9 activity in schistosomes

The activity and efficiency of CRISPR/Cas9 to edit the schistosome genome, by targeting the ω1 locus, was explored using two approaches. First, a ribonucleoprotein complex (RNP) comprised of sgRNA mixed with recombinant Cas9 endonuclease was delivered into schistosome eggs isolated from livers of infected mice (egg preparation termed ‘LE’, liver eggs) by square wave electroporation. In addition, Homology Directed Repair (HDR) of CRISPR/Cas9-induced DSBs at the *ω1* locus in the presence of a donor DNA template was investigated [38-40]. Therefore, a single stranded oligodeoxynucleotide (ssODN) of 124 nt in length was delivered to some LE as a template for HDR of chromosomal double stranded breaks (DSBs) (Fig. 1B). The ssODN included a short transgene coding for six stop codons flanked by 5’- and 3’-homology arms, each arm 50 nt in length, complementary to the genome sequence of exon 1 on both the 5′ and 3′ sides of the programmed Cas9 cleavage site (Fig. 1A, B). After 72 hours in culture, total RNA was recovered from LE to quantify the ω1expression. In a second approach, LE were maintained for 24 hours in culture medium containing pseudotyped pLV-ω1X1 virions [41] and transfected with the ssODN repair template (above) by electroporation. Specifically, the pLV-ω1 plasmid encoding Cas9 driven by the mammalian translational elongation factor 1 (tEF1) promoter, and the sgRNA (20 nt) targeting exon 1 driven by the human U6 promoter [42], was assembled in the lentiviral vector pLV-U6g-EPCG (Sigma) and termed pLV-ω1X1 (Fig. 1C).

146
147 Given that the donor ssODN included a short transgene that would facilitate genotyping, PCR
148 was performed using template genomic DNAs from the CRISPR/Cas9-treated LE [38] to reveal
149 the extent by which knock-in (KI) had occurred. A forward primer termed Smω1X1-6stp-cds-F
150 specific for the ssODN transgene was paired with three discrete reverse primers, termed Smω1-
151 R1, Smω1-R2 and Smω1-R3, at increasing distance from the predicted HDR insertion site in *ω1*
152 (Table S2). Amplicons of the expected sizes of 184, 285 and 321nt were observed in genome-
153 edited eggs but not from control eggs (Fig. 2A, B; Fig. S3), a diagnostic pattern indicative of the
154 insertion of the ssODN transgene into ω1 and, in turn, indicating that the resolution of the DSB
155 at the ω1 locus from CRISPR/Cas9 had been mediated by HDR. Amplification using a control
156 primer pair, termed Smω1-control-F/R, which spanned the predicted DSB also was carried out,
157 yielding amplicons of the expected size of 991 nt. Similar findings were observed with genome
158 editing delivered by RNPs and by LV (Fig. S3). Sanger sequence analysis of the knocked-in
159 amplicons (KI-R1, KI-R2 and KI-R3) confirmed the presence of the transgene inserted into the
160 ω1 locus at the site predicted for programmed Cas9 cleavage (Fig. 2C).

161 **Programmed mutations detected in exon 1 of *ω1***

162 The activity of CRISPR/Cas9 was first evaluated by a quantitative PCR (qPCR) approach that
163 relies on the inefficient binding of a primer overlapping the gRNA target, i.e. where mutations
164 are expected to have occurred, compared to the binding efficiency of flanking primers, i.e.
165 outside the mutated region [43, 44]. The overlapping (OVR) primer pair shared the reverse
166 primer with OUT primer (Fig. S4). Genomic DNA template was used for qPCR to quantify the
167 efficiency of CRISPR-mediated mutagenesis at the target locus; the ratio between the OVR
168 products and OUT products provides an estimate of the frequency of CRISPR-induced indels in
169 the gRNA sequence. We observed that there were 2.2, 6.3, 3.7 and 11.4% estimated indels in
170 genomic DNAs of gRNA/Cas9 RNP complex treated, gRNA/Cas9 RNA complex with ssODN
171 treated, pLV-ω1X1 treated and pLV-ω1X1 with ssODN treated samples. Differences were not
172 apparent among the control groups, untreated LE. Opti-MEM only, heated- killed pLV-ω1X1
173 with and without donor ssODN, and ssODN only.
174
175 In addition, to identify and quantify the scope and nature of the mutation(s) that arose in the
176 genome of *ω1* gene edited-eggs, we constructed amplicon NGS Illumina barcoded libraries from
177 pooled genomic DNAs of six independent exposures of LE to pLV- ω1X1 virions following by
178 transfection with the donor ssODN. The amplicon libraries were subjected to deep sequencing on
179 the MiSeq Illumina platform. Interrogation of the nature and impact of CRISPR/Cas9 at *ω1* was
180 undertaken with the CRISPResso pipeline [45]. At the outset, ~2 million reads from the
181 GENEWIZ reads of the pLV-ω1X1+ ssODN group were compared to the reference sequence,
182 which revealed numerous deletions proximal to the programmed mutation site in the
183 Smp_193860 locus (Fig. 2D). Subsequently, CRISPResso compared >56 million sequenced
184 reads to the reference sequence of the Smp_193860 locus (Table S3). The analysis revealed that
185 71% were WT (unmodified DNA) whereas 29 % reads exhibited apparent mutations (Fig. 2E)
186 across the 202 bp amplicon, with 0.13% insertions, 0.58% deletions and 28.2% substitutions
187 (sample 9 in Table S3). In contrast, in a control eggs-only sample, 76% were WT, and 24% of
188 reads exhibited apparent mutations, with 0.14% insertions, 0.33% deletions, and 24.0%
189 substitutions (Fig. 2E; sample 2 in Table S3). Thus, subtracting the rate of apparent mutations in
190 the control, we estimate that approximately 0.25% and 4.2% of reads in the experimental sample
191 carried programmed CRISPR-induced deletions and substitutions, respectively.

192 INDELs of 1-2 bp (or multiples thereof) in coding DNA cause frame-shifts, and consistent with
193 its higher rate of indels, the CRISPR-treated sample displayed a higher rate of frame-shifts
194 compared to a control eggs-only sample (2.0% for sample 9 versus 1.4% for sample 2; Table S3;
195 Fig. 2E). A caveat was that some apparent substitutions may reflect variation among the copies
196 of *ω1* rather than programmed mutations. The Illumina sequence reads revealed several common
197 variants, such as adjacent 'TA' substitutions instead of 'CC' at positions 152-153 of the
198 amplicon, which causes a change from Q to K at the amino acid level. Gene Smp_193860 has
199 'AT' at this position in the V5 assembly, as does mRNA XP_018647487.1 from the NCBI
200 database, whereas Smp_193860, Smp_184360 and Smp_179960 all have 'CC' at this position in
201 the V7 assembly (Fig. S4 panels A, B), whereas 'CC' was also found in KI fragments using
202 Sanger direct sequencing (Fig. 2C). Similarly, a second common dinucleotide substitution from
203 'AC' to 'TT' at positions 60-61 encodes a change from T to F. Both dinucleotide substitutions
204 were found together in 8% of reads in the control sample (sample 2, Table S3) and 4% of reads
205 in the treated sample (sample 9). Both these nonsynonymous substitutions are proximal to the
206 CAS-2 catalytic site, and hence may have functional significance (Fig. S2, panels C, D).
207
208 Along with the predicted NHEJ-catalyzed mutations, CRISPResso determined the rate of HDR-
209 mediated ssODN knock-in (Table S3; Fig. 2F). Here, insertion of the 24 bp transgene was
210 confirmed in 0.19% of the reads at the sgRNA programmed CRISPR/Cas9 target site (Fig. 2F;
211 sample 9 in Table S3). Some of the MiSeq reads containing the knock-in sequence also had the
212 'CC' to 'TA' substitutions at positions 152-153 and 'AC' to 'TT' substitutions at position 60-61
213 (Fig. S2; Table S3). This suggests that the indels catalyzed by NHEJ and/or KI by HDR occurred
214 in at more than one copy of *ω1,* probably Smp_193860, Smp_184360 and/or Smp_179960, and
215 perhaps all three and also even in other homologues. The qPCR approach estimated the indel
216 frequency at 11.4% in the pLV-ω1X1 with ssODN treatment group (Fig. S4), whereas
217 CRISPResso analysis of the pooled NGS reads indicated a frequency of indel mutation of <1%
218 (Table S3).

219 **Programmed gene editing reduced the expression of ω1**

220 LE transfected with RNP complexes, with or without ssODN, displayed a down regulation of the
221 ω1-specific transcript of ~45% and 81%, respectively, compared to controls ($P \leq 0.05$; $n = 11$;
222 control groups of LE were treated with Opti-MEM medium alone (mock), Cas9 only, sgRNA
223 only, ssODN only and WT-LE. Additionally, LE transduced with pLV-ω1X1 virions with or
224 without ssODN showed a reduction of the ω1-specific transcript of 67% and by 83%
225 respectively, when compared to controls (Fig. 3A). LE exposed to heat-inactivated virions with
226 ssODN, LE exposed to ssODN only, LE exposed to Opti-MEM only, and WT-LE all were
227 included as controls. Similar outcomes were seen in all biological replicates undertaken (n =11).
228 This outcome indicated that resolution of chromosomal DSB by NHEJ plus HDR provided
229 enhanced programmed gene knockout compared to NHEJ-mediated chromosomal repair alone.
230 Nevertheless, both RNPs and pLV virions efficiently delivered programmed gene editing to
231 schistosomes but pLV virions delivered enhanced performance with a stronger gene silencing, in
232 particular when the donor repair template was provided (Fig. 3A). When examined at later time
233 points (days 5 and 7 following manipulation of the LE), further reduction in ω1 abundance was
234 not apparent (Fig. 3B). We decided to investigate whether silencing of *ω1* was associated with a
235 reduction in the copy number of this multi-copy locus due to large DNA deletions as has been
236 described for other helminth species [39] A relative copy number estimation by qPCR performed

237 as described [46] did not show significant differences in the number of gene copies of ω1 among
238 the genome-edited eggs and controls (Fig. S5).
239
240 **Diminished ribonuclease activity in CRISPR/Cas9 mutated Soluble Egg Antigen**
241 **preparation (SEA)**
242 The ribonuclease activity of the ω1 glycoprotein in SEA is associated with the Th2-polarizing
243 immune response that characterizes the appearance of schistosome egg granulomata [19, 22].
244 Ribonuclease activity of SEA from control and experimental groups on substrate yeast RNA was
245 investigated following CRISPR/Cas9 programmed mutation of *ω1* mediated by the RNP and by
246 the pLV approaches with or without ssODN (genome editing condition that led to the highest
247 level of mRNA reduction) [20, 47]. Intact yeast RNA was evident in the DNase-RNase free-
248 condition (negative control), indicative of absence of RNase activity in the reagents (200 ng
249 yeast RNA at the outset). There was near complete hydrolysis of yeast RNA following exposure
250 to RNase A (positive control); ~1.4 ng RNA remained intact. Wild type SEA exhibited marked
251 RNase activity against the yeast RNA; ~70 ng RNA remained after one hour, corresponding
252 to >60% digestion. Incubation of the RNA with Δω1-SEA from the experimental groups, RNP,
253 RNP+ssODN, pLV-ω1X1, and pLV-ω1X1+ssODN, resulted ~30% substrate digestion, with
254 124, 140, 135 and 153 ng RNA remaining, respectively. All conditions for programmed genome
255 editing resulted in less digestion of the yeast RNA than for WT SEA ($P \leq 0.0001$) (Fig. 3C, D).
256 Moreover, the Δω1-SEA with programmed knock-in exhibited less RNase activity than Δω1-
257 SEA prepared without the donor ssODN repair template ($P \leq 0.01$).
258
259 **Depleting SEA of ω1 down-regulated inflammatory activities of macrophages to induce**
260 **Th2 response**
261 The ω1 ribonuclease alone is capable of conditioning human monocyte-derived dendritic cells to
262 drive Th2 polarization [22] and enhanced $CD11b^+$ macrophage [30] modulation of intracellular
263 toll like receptor (TLR) signaling. ω1 ribonuclease inhibited TLR-induced cytokine production
264 of IL-1β and shifted the TLR signaling outcome towards an anti-inflammatory posture via
265 mannose receptor (MR) and dectin [22, 48, 49]. A co-culture of a human monocytic cell line,
266 THP-1, and a human $CD4^+$ T cell line, THP-1, was employed to study the interaction of antigen
267 presenting cells and T cells [50, 51]. First, the THP-1 cells were activated with PMA for 48
268 hours, then pulsed with SEA or Δω1–SEA for 48 hours, after which the Jurkat $CD4^+$ T cells were
269 added to the wells. Thereafter, the co-culture continued for 72 hours. Th2 cytokines and other T
270 helper cells cytokines including IL-4, IL-5, IL-13, IL-2, IL-6, IL-10, TNF-α and IFN-γ were
271 quantified in culture supernatants of the co-cultured cells (Fig. 4). SEA from ω1-mutated eggs
272 stimulated reduced levels of Th2 cytokines; IL-4 and IL-5 in comparison to wild-type SEA ($P \leq$
273 0.01). There also was less IL-13 but this was not statistically significant (Fig. 4). Production of
274 IL-6 and TNF-α were reduced ($P \leq 0.01$, whereas significant differences in IL-10. IL-2 and IFN-
275 γ were not apparent between the WT- and mutant-SEA co-cultures.
276
277 **Granulomatous inflammation markedly reduced in lungs of mice injected with Δω1 eggs**
278 Following the entrapment of eggs in the intestines, liver and eventually lungs, the glycosylated
279 ω1 ribonuclease represents the principal stimulus that provokes the circumoval granuloma,
280 necessary for extravasation of the eggs [52]. A long established model of the schistosome egg
281 granuloma employs tail vein injection of eggs into mice, which leads to formation of circumoval
282 granuloma in the mouse lung [53-55]. The latter approach has been extensively employed for

283 immunopathogenesis-related studies of ω1 [16]. Accordingly, to elicit circumoval granulomas,
284 ~3,000 WT or Δω1 LE were injected into the lateral vein of the tail of BALB/c mice, and the
285 mice euthanized 10 days later. The entire left lung was removed, fixed, sectioned, and stained for
286 histological analysis (Fig. 5). Representative digital microscopic images of whole mouse lungs
287 acquired through the 2D ultra-high-resolution digital scanner from Leica Aperio Slide Scanner
288 are shown in Fig. 5, panels A-F. At low magnification (2×), severe and widespread pulmonary
289 inflammation was visible in the mice exposed to WT eggs compared to Δω1eggs. In addition,
290 more intense and dense focal circumoval inflammation was induced by WT compared to Δω1
291 eggs (Fig. 5A). Granulomas were not seen in control naïve mice not exposed to schistosome eggs
292 (Fig. 5C). At 20× magnification, considerable disparity in volume of the circumoval granulomas
293 was observed for WT versus Δω1 LE (Fig. 5A1-A2, 5D, 5E vs Figs. 5B1-B2, 5F, G). The
294 volume of granulomas surrounding single schistosome eggs was quantified; those surrounding
295 WT eggs in lungs of the mice was 18-fold greater than for ω1-mutated eggs, means 6.21×10^{-2} ±
296 1.61×10^{-3} mm^3 and $0.34\times10^{-2} \pm 0.12\times10^{-4}$ mm^3 (17-26 granulomas per mouse), respectively ($P <$
297 0.0001) (Fig. 5H). The experiment was repeated, with 3-4 mice per group, with similar findings.
298 These findings documented a marked deficiency in the induction of pulmonary granulomas by
299 the Δω1 compared to WT eggs of *S. mansoni*.

300

301 **GenBank/EMBL/DDBJ**

302 ***Database accession*** Bioproject; PRJNA415471,
303 https://www.ncbi.nlm.nih.gov/bioproject/415471. Biosample SAMN07823308; *Schistosoma*
304 *mansoni* omega1 gene editing by CRISPR/Cas9
305 SAMN07823308 • SRS2756667 • Sequencing data for the mutation profiles are available at the
306 Sequence Read Archive (SRA) accessions SRR6374209, SRR6374210.
307

308 **Discussion**

309 In the current study, programmed CRISPR/Cas9 genome editing in *Schistosoma mansoni* was
310 undertaken to investigate its feasibility in a representative platyhelminth species. Genome
311 editing was successfully achieved as evidenced by site-specific mutations in the ω1 locus in
312 chromosome 1. The chromosomal lesion induced by CRISPR/Cas9 was repaired by the non-
313 homologous end joining (NHEJ) pathway [56] in the absence of a donor oligonucleotide, and
314 was repaired by homology directed repair (HDR) when a single stranded donor oligonucleotide
315 was provided as the repair template and/or by NHEJ [57-59]. To our knowledge, this report
316 provides the first description and characterization of CRISPR/Cas programmed genome
317 engineering in schistosomes and in any species of the phylum Platyhelminthes.
318
319 At least five intact copies of ω1 are localized on chromosome 1 of *S. mansoni*, and although the
320 open reading frame and amino acid sequences of these copies are conserved, the copies of *ω1*
321 display variation in exon/intron structure (although some of these differences may be due to
322 imprecise annotation). In order to edit the *ω1* locus, we decided first to deliver the
323 CRISPR/Cas9 components to the mature egg stage (liver eggs, LE) of the schistosome since the
324 ω1 T2 ribonuclease is tightly expressed only at this stage of schistosome development [20, 27,
325 29]. The LE preparation includes a spectrum of egg development ranging from newly laid,
326 immature, fully mature and dead eggs, although the proportion of LE that is mature and ready to
327 hatch when placed in water is > 70% [11]. When released from the adult female schistosome
328 into the mesenteric veins, the schistosome ovum contains a single celled zygote surrounded by
329 30 to 40 vitelline cells [27]. By six or so days later, the miracidium within the eggshell is a
330 mobile, ciliated larva comprised of organs, tissues, muscles and nerves [25, 60-62].
331
332 Somatic genome engineering was undertaken by delivering the CRISPR/Cas9 machinery by two
333 methods to schistosome eggs recovered from livers of experimentally infected mice. First,
334 CRISPR/Cas9 was delivered as a ribonucleoprotein particle (RNP) complex consisting of
335 recombinant Cas9 from *Streptococcus pyogenes* complexed with a single guide RNA (sgRNA)
336 specific for exon 1 of the ω1 locus. The second approach was based on lentiviral virion delivery
337 where both the Cas9 and sgRNA were included as cargo in the construct. Delivery of
338 CRISPR/Cas9 by RNP, by lentiviral virions, and other methods have been thoroughly employed
339 in cells lines, tissues and entire organisms [63-66]. Immediate editing leading to DSB is an
340 advantage with delivery of RNPs in cells whereas the short half-life of the RNP components may
341 be disadvantageous. By contrast, delivery of the CRISPR components on plasmids and by viral
342 mediated infection can provide more sustained activity, transgene integration in non-dividing
343 cells, and other attributes [33, 67]. With mature schistosome eggs, LV-mediated delivery was
344 expected to increase the performance and efficiency of the somatic genome editing given that the
345 provirus integrates into the genome after infection, the transgene would be transmitted by
346 mitosis, and extended expression would be feasible. RNPs were delivered to LE by square wave
347 electroporation, an established delivery method for this developmental stage [68]. For LV, we
348 used VSVG-pseudotyped HIV virions, since the lentiviral provirus will integrate into
349 schistosome chromosomes [41]. Moreover, delivery by LV provides a hands-free approach that
350 enables scaling of gene editing and potentially to reach less accessible and/or differentiated cells.
351
352

353 Genomic DNAs recovered from ~ 10,000 CRISPR/Cas9-treated LE included many thousands of
354 copies of the schistosome genome, and in addition, several copies of the gene itself are found in
355 each genome. Analysis assisted by the CRISPResso pipeline of the deep sequence reads of
356 amplicons spanning the predicted DSB site revealed that ~6% of the reads were mutated by
357 insertions, deletions, and substitutions, with an efficiency for HDR of 0.18% insertion of the
358 donor transgene. The target locus was mutated by knock-in (KI) of a ssODN repair template
359 bearing short homology arms to mediate homology directed repair following DSB at *ω1*.
360
361 Concerning the mutation profile of CRISPR/Cas9-induced repair, the numerous substitutions
362 compared to deletions and insertions was noteworthy. On the other hand, this is a multi-copy
363 gene and some substitutions may reflect the multi-family nature of ω1. The sequenced reads
364 from the amplicon NGS libraries revealed micro- and macro-variability in the sequences at the
365 following repair of the DSB. Given that this genome editing investigation involved multicellular
366 targets, it is an example of somatic (rather than germ line) genome editing. [67]. Given also the
367 multiple copies of *ω1*, the numerous cells in each of the ~10,000 LE, the spectrum of
368 development of these eggs, the diverse mutation profile of NHEJ, and the other contributions to
369 variability (below), mosaicism of mutations was expected, i.e. some displayed HDR, some NHEJ
370 but not HDR, other cells and NHEJ and/or HDR, and many retained the wild type (non-mutated).
371 As well as the expected relative ease of access by the RNPs, virions and ssODN to the cells of
372 syncytial inner envelope compared to the cells within the miracidium, other factors may have
373 contributed to variability of CRISPR efficiency among the eggs and among the cells of a single
374 egg. Cells exposed to CRISPR/Cas9 components may not have been undergoing cell dividing;
375 HDR can proceed only at cell division, with the cell at late S phase or G2 following completion
376 of DNA replication and access to sister chromatids as the repair templates [69]. Otherwise,
377 NHEJ proceeds to repair the DSB. Whereas incubating the eggs in virions would be expected to
378 ensure that virions contacted every egg, the coverage of infection was not assessed, both for the
379 coverage by RNPs and the subsequent transduction by ssODN.
380
381 In addition to the mutations identified in the DNA we investigated their impact at the mRNA
382 level of ω1. The levels of ω1-encoding mRNA were reduced by up to 83% (relative to the
383 control), indicating that Cas9 catalyzed mutation of *ω1*, and that programmed Cas9-induced
384 double stranded chromosomal breaks had been resolved by non-homologous end joining (NHEJ)
385 and/or homology direct repair (HDR) events. The knock-in of a ssODN repair template in
386 cultured eggs induced 81-83 % reduction in *ω1*-specific mRNA levels, whereas a down
387 regulation of 67 to 83 % was observed following exposure to RNP/LV without ssODN. A
388 tentative explanation of the paradox of the >80% reduction in transcription of ω1 side-by-side
389 with <1 % efficiency in gene editing (based on NGS reads) may be tight tissue specific
390 expression of ω1, which only occurs within the syncytial 'inner envelope' of squamous,
391 epidermal-like cells surrounding the miracidium [60]. Expression of *ω1* appears to be tightly
392 developmentally regulated; based on comparison of expression in the egg to expression in the
393 miracidium, immunostaining and transmission electron microscopy of the mature egg, all or
394 most expression of ω1 takes place in the mature egg and not in immature eggs or other larval or
395 adult stages [20, 25, 27, 29, 70]. Within the mature egg, the fully developed miracidium is
396 surrounded by a squamous, syncytial epithelium termed variously as the envelope, the inner
397 envelope, or von Lichtenberg's envelope [25, 27, 60, 61]. This syncytial layer is metabolically
398 active [27], and likely the site of synthesis of T2 ribonuclease ω1 that is released from the egg

399 [25, 27, 29], along with other secreted/ excreted proteins that help facilitate egress of the egg
400 from the blood vessels and through the wall of the intestine [27]. The virions may not have
401 infected many of the cells within mature eggs, because after entry into the egg the virus would be
402 expected to contact the syncytial envelope, rather than traveling further to directly contact cells
403 of the miracidium. That is, the efficiency of gene editing may not have been high across all cells
404 of an egg but may (due to ease of access to certain cells) have had highest efficiency in those
405 cells in which ω1 is expressed. This may explain the large reduction in *ω1* transcripts in the
406 CRISPR-treated eggs relative to the control eggs.

407 The inconsistency between the substantially reduced mRNA levels and the lower frequency of
408 mutations observed in MiSeq sequence data might also reflect CRISPR/Cas9 induced large size
409 deletions (>500 bp) that would include the primer sites and hence not be detected by the
410 sequencing approach (i.e. PCR-amplicon next generation sequencing) as reported in
411 *Strongyloides stercoralis* [39]. Large deletions would explain the transcript-knock down due to a
412 reduction in the copy number of the target gene. However, based on the qPCR findings
413 differences in *ω1* copy number were not evident among CRISPR/Cas9-treated LE and controls.
414 Notwithstanding, indels arising following Cas9-catalyzed DSBs frequently result in frameshift
415 mutations that, in turn, lead to nonsense-mediated mRNA decay (NMD) of the mutant transcript
416 [71], which effectively knocks out the gene [72].

417 Whereas wild-type SEA polarized Th2 cytokine responses including IL-4 and IL-5 in human
418 monocyte/T cell co-cultures, significantly reduced levels of these cytokines were observed when
419 the cells were exposed to ω1-mutated SEA. Moreover, following introduction of eggs into the
420 tail vein of mice, pulmonary circumoval granulomas were substantially reduced in size around
421 Δω1 eggs compared to granulomas and the inflammation provoked by wild type eggs. Whereas
422 this outcome extends earlier findings using lentiviral transduction of eggs of *S. mansoni* to
423 deliver microRNA-adapted short hairpin RNAs aiming to silence expression of ω1 [16], the
424 reduction in granuloma volume was far more prominent in the present study. Residual
425 granulomas around mutant eggs could be due to prostaglandin E_2 levels [73], in addition to
426 incomplete disruption of all copies of *ω1*. Given that the T2 ribonuclease ω1 is the principal type
427 2-polarizing protein among egg-secreted proteins [19, 20], our findings of a phenotype
428 characterized by absent or diminutive granulomas provide functional genomics support to this
429 earlier advance [22].
430
431 The findings confirmed that somatic genome editing of the schistosome egg, lead to knockout of
432 the ω1 T2 ribonuclease, and mosaicism of mutant and wild type cells within the schistosome
433 egg. The Cas9 nuclease catalyzes programmed cleavage of schistosome chromosomes, and the
434 nuclease and sgRNA can be provided from schistosome cells following infection with lentiviral
435 virions. The Cas9 gene edited schistosome eggs remained viable but exhibited loss of function of
436 ω1. Programmed mutation of *ω1* using CRISPR/Cas9 not only achieved our aim to establish
437 applicability and tractability of genome editing for functional genomics of schistosomes but also
438 demonstrated manipulation of a gene expressed in the schistosome egg, the developmental stage
439 of the pathogen central to the pathophysiology and immunobiology of schistosomiasis. This
440 report provides a blueprint that can be applied to other schistosome genes, and those of
441 trematodes and platyhelminths at large. In addition, future studies that combine pseudotyped
442 virions to deliver transgene-encoded programmed genome editing to the schistosome germ line,
443 to derive lines of mutant parasites [11] would enable more comprehensive understanding of the

444 pathogenesis and pathophysiology of this neglected tropical diseases pathogen that will lead to
445 the discovery of novel strategies for control.
446

447 **Materials and Methods**

448 **Ethics statement**

449 Mice experimentally infected with *S. mansoni*, obtained from the Biomedical Research Institute,
450 Rockville (BRI), MD were housed at the Animal Research Facility of the George Washington
451 University Medical School, which is accredited by the American Association for Accreditation
452 of Laboratory Animal Care (AAALAC no. 000347) and has an Animal Welfare Assurance on
453 file with the National Institutes of Health, Office of Laboratory Animal Welfare, OLAW
454 assurance number A3205-01. All procedures employed were consistent with the Guide for the
455 Care and Use of Laboratory Animals. The Institutional Animal Care and Use Committee of the
456 George Washington University approved the protocol used for maintenance of mice and
457 recovery of schistosomes. Studies with BALB/c mice involving tail vein injection of schistosome
458 eggs and subsequent euthanasia using overdose of sodium pentobarbitone was approved by the
459 IACUC of the Biomedical Research Institute (BRI), protocol 18-04, AAALAC no. 000779 and
460 OLAW no. A3080-01.

461

462 **Schistosome eggs**

463 Mice were euthanized seven weeks after infection with *S. mansoni*, livers were removed at
464 necropsy, and schistosome eggs recovered from the livers, as described [74]. The eggs termed
465 'LE' were maintained in RPMI medium supplemented with 10% heat inactivated fetal bovine
466 serum (FBS), 2% streptomycin/penicillin and protease inhibitor cocktail (Sigma) at 37°C under
467 5% CO_2 in air [75, 76]. Polymyxin B to 10 μg/ml was added to the cultures twice daily to
468 neutralize lipopolysaccharide (LPS) [77]. Soluble egg antigen (SEA) was prepared from these
469 eggs, as described [23, 53]. In brief, the homogenate of eggs in 1×PBS containing protease
470 inhibitor cocktail (Sigma) was frozen and thawed twice, clarified by centrifugation at 13,000
471 rpm, 15 min, 4°C, the supernatant passed through a 0.22-μm pore size membrane. Protein
472 concentration of the supernatant (SEA) were determined by the Bradford Protein Assay [78] and
473 aliquots of the SEA stored at -80°C.

474

475 **Guide RNAs, Cas9, and single stranded DNA repair template**

476 Single guide RNA (sgRNA) was designed using the web-based tools at
477 http://bioinfogp.cnb.csic.es/tools/breakingcas/ [79] to predict cleavage sites for the *Streptococcus*
478 *pyogenes* Cas9 nuclease within the genome of *S. mansoni*. The sgRNA targeted exon 1 of the ω1
479 gene, Gene ID Smp_193860, www.genedb.org, residues 164-183, adjacent to the protospacer
480 adjacent motif, AGG (Fig. 1A). This is a multi-copy gene with five copies of ω1 located in
481 tandem on chromosome 1. The Smp_193860 copy of ω1 includes four exons interspersed with
482 three introns (2,569 nt) (Fig. 1A). Synthetic gRNA (sgRNA), ω1-sgRNA was purchased from
483 Thermo Fisher Scientific (Waltham, MA). A double stranded DNA sequence complementary to
484 the sgRNA was inserted into lentiviral gene editing vector, pLV-U6g-EPCG (Sigma), which
485 encodes Cas9 from *S. pyogenes* driven by the eukaryotic (human) translation elongation factor 1

486 alpha 1 (tEF1) promoter and the sgRNA driven by the human U6 promoter (Fig 1C). (The pLV-
487 U6g-EPCG vector is tri-cistronic and encodes the reporter genes encoding puro and GFP, in
488 addition to Cas9, using the 2A peptide approach [80].) This gene-editing construct, targeting
489 exon 1 of *ω1* Smp_193860, was termed pLV-ω1X1. A single stranded oligodeoxynucleotide
490 (ssODN), which included homology arms of 50 nt each in length at the 3' (position 131-180 nt)
491 and 5'(181-230 nt) flanks and a small transgene (5'-TAAGTGACTAGGTAACTGAGTAG-3',
492 encoding stop codons (six) in all reading frames) (Fig. 1B), was synthesized by Eurofin
493 Genomics (KY, USA). An oligonucelotide primer of the same 24 nt sequence was also employed
494 as the forward primer to investigate the presence of CRISPR/Cas9-programmed insertion of the
495 transgene [81] (Table S2).
496

497 **Transfection of schistosome eggs with a Cas9/guide RNA complex**

498 For the ribonucleoprotein (RNP) complex of the ω1-sgRNA and recombinant Cas 9, three μg ω1-
499 sgRNA and 3 μg Cas9-NLS nuclease (Dharmacon, Lafayette, CO) were mixed in 100 μl Opti-
500 MEM (Sigma) to provide 1:1 ratio w/w RNP. The mixture was incubated at room temperature
501 for 10 min, pipetted into a 4 mm pre-chilled electroporation cuvette containing ~10,000 LE in
502 ~150 μl Opti-MEM, subjected to square wave electroporation (one pulse of 125 volts, 20
503 milliseconds) (BTX ElectroSquarePorator, ECM830, San Diego, CA), thereafter incubated for 5
504 min at room temperature, and subsequently maintained at 37°C, 5% CO_2 in air for 3, 5 and 7
505 days. To investigate whether homology-directed repair (HDR) could catalyze the insertion of a
506 donor repair template, 3 μg ssODN was mixed with RNP and the LE before electroporation. In
507 the second approach (above), the ssODN was delivered to LE by electroporation at ~24 hours
508 after lentiviral transduction of the LE. The eggs were collected 3, 5 and 7 days later and genomic
509 materials recovered from LE. The negative controls included LE subjected to electroporation in
510 the presence of only Opti-MEM (mock), only Cas 9, only sgRNA, and only ssODN.
511

512 **Transduction of schistosome eggs with lentiviral particles**

513 *Escherichia coli* Zymo 5α (Zymo Research) cells were transformed with lentiviral plasmid pLV-
514 ω1X1 and cultured in LB broth in 100 μg/ml ampicillin at 37°C, agitated at 225 rpm for ~18
515 hours, after which plasmid DNA was recovered (GenElute Plasmid purification kit, Invitrogen).
516 A lentiviral (LV) packaging kit (MISSION, Sigma-Aldrich) was used to prepare LV particles in
517 producer cells (human 293T cell line). In brief, 2.3×10^5 of 293T cells/well were seeded 6-well
518 tissue culture plate in DMEM supplemented with 10% heat- inactivated fetal bovine serum
519 (FBS), 2 mM L-glutamine, 2% penicillin/streptomycin and cultured at 37°C, 5% CO_2 for 18
520 hours. The producer cells were transfected using FUGENE 6 (Promega) with pLV-ω1X1 and LV
521 packaging mix containing two additional plasmids, one to express HIV structural and packaging
522 genes and the other to express the pseudotyping envelope protein, VSVG (vesicular stomatitis
523 virus glycoprotein). Subsequently, the transfection mixture (37.5 μl; 500 ng plasmid DNA, 4.6 μl
524 packaging mix, 2.7 μl of FUGENE 6 in Opti-MEM) was dispensed drop wise into each well on
525 the plate. Sixteen hours later, the media were removed from the transfected cells, replaced with
526 pre-warmed complete DMEM, and cells cultured for 24 hours. The supernatant, containing
527 VSVG-pseudotyped LV particles was filtered through 22 μm pore size membranes [41], and
528 stored at 4°C. Additional pre-warmed complete DMEM was added to the well, for culture for a
529 further 24 hours. The supernatant was collected, as above, and added to the first supernatant, and

530 concentrated (Lenti-X concentrator, Takara Bio, Mountain View, CA). Virion titer was
531 estimated by two methods: first, by use of Lenti-X-GoStix (Takara Bio) to establish the presence
532 of functional virions at $>10^5$ infectious units (IFU)/ml, and second, by reverse transcriptase assay
533 [41, 82] to quantify levels of active virions. Virions with counts of $\sim 4\times10^6$ count per minute
534 (cpm)/ml were aliquoted and stored at -80°C.

535 To transduce LE with LV, ~10,000 eggs were incubated for 24 hours in complete DMEM
536 containing 500 µl of $\sim 4\times10^6$ cpm/ml VSVG-LV virions. Thereafter, the LE were washed three
537 times in 1×PBS and transfected with ssODN by square wave electroporation or further steps. LV
538 virions heat-killed by incubation at 70°C for two hours [41] with subsequent transfection with
539 the ssODN, transfection with ssODN in the absence of virions, and Opti-MEM only, all served
540 as negative controls.

541

542 **PCR amplification of diagnostic transgene to detect knock-in into exon 1 of ω1**

543 For each DNA sample, four separate PCR assays using four distinct primer pairs (Table S2) were
544 carried out. The first ω1 primer pair, to amplify locations 107-1,097 nt of Smp_193860, was
545 served as a positive control for the presence of genomic DNA with the Smp_193860 copy of *ω1*.
546 The other primer pairs shared one forward primer complementary to the knock-in 24 nt transgene
547 with three reverse primers, Sm ω1-R1, -R2 and -R3 at positions 346-364, 446-465 and 482-501
548 nt, respectively, bind complementary to three sites downstream the ω1 target site DSB (Fig. 2A;
549 Table S2) [81]. The PCR mix included 10 µl Green GoTaq DNA polymerase mix (Promega)
550 with 200 nM of each primer and 10 ng genomic DNA. Thermal cycling conditions involved
551 denaturation at 95°C, 3 min followed by 30 cycles of 94°C, 30 sec, 60°C, 30 sec and 72°C, 30
552 sec and a final extension at 72°C for 5 min. Amplicons were visualized following agarose gel
553 electrophoresis (1.2% agarose/TAE), and those of the expected sizes were recovered from gels
554 and cloned into pCR4-TOPO (Thermo Fisher). *E. coli* Zymo 5α competent cells were
555 transformed with the ligation products, three single colonies of each transformant on LB
556 agar/ampicillin were amplified, and insert sequences determined to confirm the presence and
557 knock-in of the transgene (Fig. 1C).

558

559 **Illumina sequencing**

560 Pooled LE DNA samples from six independent KI experiments of pLV-ω1X1 with ssODN were
561 used as the template to amplify the on-target DNA fragment using MiSeq primers (Fig. 2A) with
562 High Fidelity *Taq* DNA polymerase (Thermo Fisher). The expected size of the amplicon
563 flanking predicted DSB was 205 bp. Amplicons of this size were purified by Agencourt AMPure
564 XP (Beckman Coulter) and prepared for sequencing using the Illumina MiSeq platform. Paired-
565 end read libraries were constructed using the QIAseq 1-Step Amplicon Library Kit (Qiagen) and
566 GeneRead Adaptor I Set A 12-plex (Qiagen) using discrete index adaptors. These libraries were
567 pooled, and the library pool was quantified using the QIAseq Library Quant System (Qiagen).
568 Paired end, MiSeq Illumina sequencing of the pooled amplicons was carried out either at
569 GENEWIZ (South Plainfield, NJ) and/or the Wellcome Genome Center.

570 Samples (10) (Table S3) were multiplexed and each run on four MiSeq lanes. After sequencing,
571 the fastq files for each particular sample were merged. Samples 7 and 9 were prepared by a

572 slightly modified approach (higher PCR anneal temperature) and in a separate laboratory than
573 the other libraries, and (for as yet unclear reason) included an extra 10 bp at the start of the
574 MiSeq sequences, 'GTTTTAGGTC', present upstream of the 5' primer in the genomic DNA).
575 We trimmed this sequence from the reads using cutadapt v1.13 [83]. To detect HDR events,
576 CRISPResso v1.0.9 [45, 84] was employed using a window size of 500 bp (-w 500) with the
577 reference amplicon according to gene *Smp_193860* in the *S. mansoni* V7 assembly, and with the
578 --exclude_bp_from_left 25 and --exclude_bp_from_right 25 options in order to ignore the (24
579 bp) primer regions on each end of the amplicon when indels are being quantified. A window size
580 of 500 nt was employed include the entire amplicon. In order to search for HDR events,
581 CRISPResso checked for HDR events (using –e and –d options) in treatment groups including
582 controls. To infer frameshifts using CRISPResso the –c option was used, giving CRISPResso the
583 coding sequence from positions 42-179 of the amplicon. To confirm the insertions of the knock-
584 in sequences reported by CRISPResso (column L in Table S3), we took all insertions of 20-28 bp
585 reported by CRISPResso, and calculated their percent identity to the expected knock-in sequence
586 using ggsearch v36.3.5e in the fasta package [85], and an insertion was considered 'confirmed' if
587 it had ≥75% identity to the expected knock-in sequence.
588

589 **Copy number estimation for ω1**

590 A quantitative PCR to estimate the relative copy number of *ω1* was performed using Kapa qPCR
591 mastermix SYBRfast (KK4602) on 1 ng of gDNA templates isolated from control and test
592 samples, in 20 µl volumes. Primer pair OMGgRNA1F and OMGgRNA1R was used to amplify
593 the ω1 gRNA target region and SmGAPDH (Smp_056970) as reference single-copy gene
594 (primers shown in Table S2). The PCR efficiencies for primer pairs were estimated by titration
595 analysis to be 100% ±5 [86] and qPCRs were performed in triplicate, using 96-well plates, with a
596 denaturation step at 95°C of 3 min followed by 40 cycles of 30 s at 95°C and 30 s at 55°C, in
597 thermal cycler fitted with a real time detector (StepOnePlus, Applied Biosystem). The relative
598 quantification assay $2^{-\Delta\Delta Ct}$ method [87] was used to ascertain the relative copy number of *ω1*.
599 Relative ω1 copy number in CRISPR/Cas9 treated groups reflects the fold change of *ω1* copy
600 number normalized to the Sm GAPDH reference gene and relative to the untreated control group
601 (calibrator sample with relative *ω1* copy number = 1) [46].
602

603 **Analysis of RNase activity of ω1**

604 A stock solution of yeast RNA (Omega Bio-tek, Norcross, GA) was prepared at 1.0 µg/µl, 50
605 mM Tris-HCl, 50 mM NaCl, pH 7.0. Yeast RNA (200 ng) was incubated with 2 µg SEA from
606 control and experimental groups individually at 37°C for 60 min. (SEA investigated here, named
607 Δω1-SEA, was extracted LE transduced with pLV- ω1X1 virions and ssODN, pooled from six
608 biological replicates.) RNase A, an endoribonuclease from bovine pancreas (Thermo Fisher)
609 served as a positive control enzyme whereas yeast RNA in reaction buffer only served as the
610 negative control. The RNase activity of ω1 in wild type SEA or Δω1-SEA was analyzed by
611 visualizing and quantifying the substrate that remained following enzymolysis by agarose gel
612 electrophoresis and staining with ethidium bromide. The yeast RNA digestion by control SEAs
613 or Δω1-SEA were set up in triplicates, with quantity of residual RNA determined by
614 densitometry [47].

615

616 **Schistosome egg induced primary pulmonary granuloma in mice**

617 For induction of circumoval, egg-induced granulomas in the lungs of mice, 8 week old female
618 [25] BALB/c mice were injected with 3,000 WT egg or Δω1-egg or 1×PBS as negative control
619 by tail vein, as described [55]. The mice (6-9 mice/group) were euthanized 10 days later. For
620 histopathological assessment of granuloma formation, the left lung was removed at necropsy and
621 fixed in 10% formalin in pH 7.4 buffered saline for 24 hours, after which it was dehydrated in
622 70% ethanol, and clarified in xylene. The fixed lung tissue was embedded in paraffin and
623 sectioned at 4-µm-thickness by microtome [55]. Thin sections of the left lung lobe were mounted
624 on glass slides and fixed at 58-60°C. Subsequently, rehydrated sections were stained with
625 hematoxylin-eosin (H&E) for evaluation of inflammatory infiltrates and cellularity of
626 granulomas. The longest (R) and shortest (r) diameters of each granuloma containing a single
627 egg were measured with an ocular micrometer, and the volume of the granuloma calculated
628 assuming a prolate spherical shape, using $4/3\ \pi\ Rr^2$ [25]. All granulomas in all slides from the left
629 lung of the mice, 15 slides per treatment group, were measured, in total >100 granulomas from
630 each treatment group. Digital images were obtained using a 2D glass slide digital scanner
631 (Aperio Slide Scanner, Leica Biosystems, Vista, CA), and examined at high magnification using
632 the Aperio ImageScope (Leica) software [54, 88].
633

634 **Macrophage polarization by WT or Δω1-SEA and T-cell activation *in vitro***

635 Human monocytic THP-1 cells were maintained in Roswell Park Memorial Institute medium
636 (RPMI) 1640 with L-glutamine, HEPES (Thermo Fisher Scientific) containing 10% (v/v) FBS
637 with 4 mM glutamine, 25 mM HEPES, 2.5 g/L D-glucose at 37°C in 5% CO_2 in air. THP-1 cells
638 were non-adherent cells. In a 6-well plate, THP-1 monocytes (3×10^5 cells in each well) were
639 differentiated into macrophages (MΦ) by incubation in 150 nM phorbol 12-myristate 13-acetate
640 (PMA) (Sigma) for 48 hours [89]. MΦ were treated with SEA (50 ng/ml) or Δω1-SEA (50
641 ng/ml) (from LE transduced with pLV-ω1X1 virions and ssODN) for 48 hours. The SEA or
642 Δω1-SEA treated MΦ were collected and processed for RNA extraction to examine cytokine
643 transcription. To investigate macrophage and T cell interactions, MΦ cells were pulsed with
644 SEA or Δω1-SEA and thereafter co-cultured with Jurkat (human $CD4^+$) T cells. Nine $\times10^5$
645 Jurkat cells were added to MΦ and incubated for an additional 72 hours. Cell-free supernatants
646 from the co-cultures were collected to quantify secretion of T helper cell cytokines including IL-
647 4, IL-5, IL-13, IL-10, TNF-α, IL-6, IL-2 and IFN-γ by enzyme linked immunosorbent assay
648 (ELISA) (Qiagen) [90]. The ELISA test was performed using three biological replicates, with
649 positive control for each analytes provided in the kit (Qiagen).

650

651 **Differential gene expression for ω1 mRNA and cytokine mRNAs**

652 Total RNAs from either schistosome were extracted using the RNAzol RT reagent (Molecular
653 Research Center, Inc), which eliminates contaminating DNA [91]. A NanoDrop ND-1000
654 spectrophotometer was used for the RNA concentration and purity ($OD_{260/280}$ ~2.0). RNA (500
655 ng) from was reverse transcribed using iScript Reverser Transcript (Bio-Rad) and the first strand
656 cDNA was employed as template for qPCR using SsoAdvanced Universal SYBR Green
657 Supermix (Bio-Rad) and run in triplicates by iQ5 Real time PCR instrument (Bio-Rad).

658 To evaluate the levels of ω1 transcripts, RT-qPCR reaction mixtures included 2 μl first stand
659 cDNA, 5 μl SsoAdvanced universal SYBR Green Supermix, and 300 nM schistosome gene
660 specific primers. Table S2 provides details of the oligonucleotide primers. Thermal cycling
661 conditions were denaturation at 95°C for 30 sec, 40 amplification cycles each consisting of
662 denaturation at 95°C for 15 sec, annealing/extension at 60°C for 30 sec, and a final melting
663 curve. The output was analyzed employing the iQ5 software. The relative expression of genes
664 was calculated using ΔΔCt method and normalized to either schistosome GAPDH expression
665 [87]. Data are presented as transcript levels (three replicates) compared to the WT (100%) LE,
666 and fold change reported as mean relative expression ± SD.

667

668 **Statistics**

669 Means for experimental groups were compared to controls by one-way ANOVA, and, where
670 appropriate, by a two-tailed Student's *t*-test or Welsh's *t*-test (GraphPad Prism, La Jolla, CA). *P*
671 values of ≤ 0.05 were considered to be statistically significant.

672 **Acknowledgements**

673 We thank Dragana Jankovic, Alan Sher, Thomas Wynn, Michael Bukrinsky, Larisa Dubrovsky,
674 Arnon Jurberg, Robert Thompson, Meredith Brindley and Luca Pinello for advice and technical
675 assistance. Schistosome-infected mice and snails were provided by the NIAID Schistosomiasis
676 Resource Center of the Biomedical Research Institute, Rockville, Maryland through NIH-NIAID
677 Contract HHSN272201000005I for distribution through BEI Resources. These studies were
678 supported by Wellcome Trust Strategic Award number 107475/Z/15/Z (Hoffmann, K.F.,
679 Principal Investigator), award R21AI109532 (GR, PJB) award from NIAID, National Institutes
680 of Health, and in part by generous support from MaxMind Inc./ TJ Mather.

681

682 **Figure legends**
683
684 **Figure 1. Genomic structure of the locus encoding ω1 (omega-1) in the genome of**
685 ***Schistosoma mansoni,* and CRISPR/Cas9 encoding construct and guide RNA.** Exon-intron
686 map of the copy of ***ω1*** at GeneDB Smp_193860, showing the position of its four exons, three
687 introns and flanking region spanning 2,569 bp on chromosome 1 (panel **A**). Nucleotide sequence
688 in exon 1 indicating location and sequence of gRNA target site, predicted double stranded break
689 (DSB) (arrow), protospacer adjacent motif (PAM) (AGG, blue box), and 124-nucleotide
690 sequence of the single stranded DNA donor template provided for DSB repair by homologous
691 recombination. Homology arms of 50 nt span a central 24 nt of six-stop-codon transgene (**B**).
692 Linear map of pLV-ω1X1 showing position of regulatory and coding regions for CRISPR/Cas9
693 editing; the positions of human U6 promoter to drive gRNA, translational elongation factor EFα-
694 1 promoter driving Cas9 from *Streptococcus pyogenes*, and the left and right long terminal
695 repeats of the lentiviral vector derived from HIV-1 (**C**).
696
697 **Figure 2. Programmed chromosomal break at *ω1* locus repaired by homologous**
698 **recombination from donor template.** Schematic diagram to indicate positions of primer
699 binding sites (blue arrows), with the foreign gene cassette as the forward primer (Smω1X1-6-
700 stop codons cassette-F) paired with three discrete reverse primers, Smω1-R1, Smω1-R2 and
701 Smω1-R3 from the *ω1* locus and a primer pair for target amplicon NGS library amplification;
702 miSeq-F and miSeq-R (panel **A**). The control PCR amplicon was generated using the Sm**ω**1-
703 control-F and –R primers. The green box shows the location of 5' and 3' homology arms, red
704 box and arrow indicate the stop codon bearing transgene. **B**, PCR products visualized in ethidium
705 bromide-stained agarose gel demonstrating Cas9-catalyzed target site-specific insertional
706 mutagenesis in exon 1 of the *ω1* gene. Evidence for transgene knocked-in into programmed
707 target site revealed by amplicons of the expected sizes in lanes R1, R2 and R3, of 184, 285 and
708 321 bp, respectively (arrows at left) spanned the mutated site in the genomic DNAs pooled from
709 schistosome eggs, including a positive control flanking the insert site (991 bp). The control
710 DNA result shown in this gel was isolated from heat inactivated-pLV-ω1X1+ssODN treated LE.
711 Similar findings were obtained when programmed gene editing was executed by lentiviral virion-
712 delivered Cas9 and *ω1*-gRNA transgenes and by ribonucleoprotein complex (RNP) delivered by
713 square wave electroporation (supporting information). The non-KI control groups (sgRNA only,
714 heat inactivated pLV-ω1X1 only, ssODN only) showed similar results, with no amplicons by
715 stop cassette-KI primers with R1, R2 or R3 (Fig. S4). **C**, Multiple sequence alignments
716 confirmed the presence of the 24 nt transgene inserted precisely into the exon 1 of ω1 locus from
717 KI-R1, -R2 and -R3 fragments comparing with *ω1* wild type (WT). The white box on ω1-WT
718 indicates the absence of the transgene sequence and white boxes on KI-R1, -R2 and –R3
719 fragments show locations of substitutions relative to the other *ω1* copies (Smp_184360): 2 bp
720 (AT to CC) mismatches at positions 253-254 nt. All three contained the (knock-in) insertion
721 sequences (white box), which was the targeted mutation of the *ω1* gene. **D-F.** Illumina deep
722 sequence analysis of amplicon library from eggs of *S. mansoni* revealed Cas9 induced on-target
723 repair of programmed gene mutation of the ω1 locus by deletions, insertions, and substitutions
724 by CRISPResso analysis. **D**. Frequency distribution of position dependent deletions and deletion
725 sizes, which vary from point mutations to more than 20 bp around the DSB. The dotted line
726 indicates the predicted site of the programmed double stranded break. **E.** Frequency of frameshift
727 versus in-frame mutations reported by CRISPResso**.** This shows the fraction of all mutations

728 (INDELs and substitutions) in coding region (positions 42-179) of the amplicon that cause
729 frameshifts (i.e. indels of 1-2 bp, or multiples thereof). Here (a) is sample 2 (control), which only
730 contained eggs, and (b) is sample 9, which was treated with lentivirus and ssODN (CRISP-
731 treated). Findings for all control and treated samples are provided in Table S3. **F.** Insertions of
732 the knock-in sequence. The y-axis is the number of amplicon reads containing an insertion of the
733 knock-in sequence (with ≥75% identity to it), and the x-axis is the position of the insertion in the
734 reference amplicon. The expected Cas9 cut site is between positions 102 and 103. Samples 3, 7
735 and 9 are independent amplicon libraries (technical replicates) made from the same sample of six
736 biological replicates treated with lentivirus and ssODN. The insert shows a sequence logo,
737 created using WebLogo [92], of the sequences of the 3,826 sequence reads from samples 3, 7
738 and 9, with insertions of 24 bp at position 102, showing that most match the expected knock-in
739 sequence, TAAGTGACTAGGTAACTGAGTAGC.
740
741 **Figure 3. Reduction of ω1 transcript and ribonuclease T2 activity after ω1 genome editing**
742 **by CRISPR/Cas9.** Panel **A.** ω1 mRNA abundance was reduced up to ~ 70% after genome
743 editing by sgRNA/Cas9 complex and lentivirus systems, and markedly reduced >80% with the
744 addition of ssODN as the DNA repair donor. The % ω1 transcripts represented mean ±SD, 11
745 biological replicates, at three days following CRISPR/Cas manipulation; asterisks **** indicate
746 statistical significance at $P \leq 0.0001$ (n=11), one-way, multiple comparison ANOVA. **B.** Stable
747 reduction of *ω1* transcripts at days 5 and 7 after treatment (three biological replicates) in four
748 experimental groups; RNP (black), RNP + ssODN (red), pLV-ω1X1 (green), pLV-ω1X1 +
749 ssODN (blue). **C, D.** Reduction of RNase activity, assessed by hydrolysis of yeast RNA [41].
750 Residual yeast following exposure to SEA, visualized after gel electrophoresis; lane 1, buffer
751 (negative control); 2, RNase A; 3-8, WT SEA and other control SEAs; 9-12, Δω1-SEA from
752 RNP, RNP + ssODN, pLV-ω1X1 and pLV-ω1X1 + ssODN, respectively (C). Intact yeast RNA
753 (nanograms) remaining following incubation with SEA, mean ±SD (n = 6). Significantly more
754 RNA remained following incubation with Δω1-SEA in all groups, RNP, RNP+ssODN, pLV-
755 ω1X1 and pLV-ω1X1+ssODN treated SEA) (blue) than in the WT SEA controls ($P \leq 0.0001$).
756 Moreover, among the gene edited experimental groups, more RNA remained where donor
757 template was introduced at the same time as RNP or pLV-ω1X1 virions ($P \leq 0.01$). Differences
758 were not apparent among WT SEA control groups (D).
759
760 **Figure 4. Reduced Th2 cytokine production following treatment with Δω1-SEA.** Panel **A.**
761 Reduction in Th2 cytokines IL-4 and IL-5 but not IL-13 [93, 94] following pulsing of MΦ
762 (PMA induced-THP-1 cells) with Δω1-SEA prior to co-culture with human $CD4^+$ T cells (Jurkat
763 cell line) compared with WT-SEA pulsed-MΦ (top panels). In addition, levels of IL-6 and TNF-
764 α were reduced where MΦ were first pulsed with Δω1-SEA but not WT SEA. Differences were
765 not evident for IL-10. The assay was carried out in triplicate. $P < 0.0001$, ≤ 0.0001, 0.0038 and
766 0.0252 indicated as ****, ***, ** and *, respectively (one way ANOVA, multiple comparison).
767
768 **Figure 5. Pulmonary circumoval granulomas revealed attenuated granulomatous response**
769 **to Δω1 schistosome eggs.** Schistosome eggs (~3,000 eggs) that had been transduced with
770 lentivirus virions encoding *ω1*-specific sgRNA and Cas9 in tandem with ssODN, were
771 introduced via the tail vein into mice. The mice were euthanized 10 days later; thin sections of
772 the left lung were stained with H&E, and circumoval granulomas counted and measured.
773 Representative 2D scanned micrographs of granulomas inoculated with WT eggs (panel **A**) (2×

774 magnification) and 20× magnification (A1 and A2), and with Δω1 eggs; **B** (2×), B1 and B2
775 (20×). **C**, Control mouse lung. **D, E** Individual control egg induced-granuloma that were counted
776 assessed for granuloma volume. **F, G**, Δω1 egg induced-granuloma. All single egg induced-
777 granuloma from WT and Δω1 eggs were measured and granuloma volume estimated [25]. **H**
778 presents scatter plots of the volume (mm^3) for individual granuloma, with mean ± SEM (red).
779 Granulomas induced by Δω1 eggs were far smaller than those surrounding WT eggs (Welch's *t*-
780 test, $P \leq 0.0001$, $n > 100$).
781

782 **References**

783 1. Gryseels B, Polman K, Clerinx J, Kestens L: **Human schistosomiasis.** *Lancet* 2006,
784 **368:**1106-1118.
785 2. Hotez PJ, Brindley PJ, Bethony JM, King CH, Pearce EJ, Jacobson J: **Helminth**
786 **infections: the great neglected tropical diseases.** *J Clin Invest* 2008, **118:**1311-1321.
787 3. Hotez PJ, Alvarado M, Basanez MG, Bolliger I, Bourne R, Boussinesq M, Brooker SJ,
788 Brown AS, Buckle G, Budke CM, et al: **The global burden of disease study 2010:**
789 **interpretation and implications for the neglected tropical diseases.** *PLoS Negl Trop*
790 *Dis* 2014, **8:**e2865.
791 4. Colley DG, Bustinduy AL, Secor WE, King CH: **Human schistosomiasis.** *Lancet* 2014,
792 **383:**2253-2264.
793 5. Berriman M, Haas BJ, LoVerde PT, Wilson RA, Dillon GP, Cerqueira GC, Mashiyama
794 ST, Al-Lazikani B, Andrade LF, Ashton PD, et al: **The genome of the blood fluke**
795 **Schistosoma mansoni.** *Nature* 2009, **460:**352-358.
796 6. Schistosoma japonicum Genome S, Functional Analysis C: **The Schistosoma japonicum**
797 **genome reveals features of host-parasite interplay.** *Nature* 2009, **460:**345-351.
798 7. Young ND, Jex AR, Li B, Liu S, Yang L, Xiong Z, Li Y, Cantacessi C, Hall RS, Xu X, et
799 al: **Whole-genome sequence of Schistosoma haematobium.** *Nat Genet* 2012, **44:**221-
800 225.
801 8. Lepesant JM, Grunau C, Cosseau C: **Towards an understanding of the epigenetics of**
802 **schistosomes: a comparative epigenomic study.** *Mem Inst Oswaldo Cruz* 2011,
803 **106:**823-830.
804 9. Geyer KK, Rodriguez Lopez CM, Chalmers IW, Munshi SE, Truscott M, Heald J,
805 Wilkinson MJ, Hoffmann KF: **Cytosine methylation regulates oviposition in the**
806 **pathogenic blood fluke Schistosoma mansoni.** *Nat Commun* 2011, **2:**424.
807 10. Vanderstraete M, Gouignard N, Cailliau K, Morel M, Hahnel S, Leutner S, Beckmann S,
808 Grevelding CG, Dissous C: **Venus kinase receptors control reproduction in the**
809 **platyhelminth parasite Schistosoma mansoni.** *PLoS Pathog* 2014, **10:**e1004138.
810 11. Rinaldi G, Eckert SE, Tsai IJ, Suttiprapa S, Kines KJ, Tort JF, Mann VH, Turner DJ,
811 Berriman M, Brindley PJ: **Germline transgenesis and insertional mutagenesis in**
812 **Schistosoma mansoni mediated by murine leukemia virus.** *PLoS Pathog* 2012,
813 **8:**e1002820.
814 12. Protasio AV, Tsai IJ, Babbage A, Nichol S, Hunt M, Aslett MA, De Silva N, Velarde GS,
815 Anderson TJ, Clark RC, et al: **A systematically improved high quality genome and**
816 **transcriptome of the human blood fluke Schistosoma mansoni.** *PLoS Negl Trop Dis*
817 2012, **6:**e1455.
818 13. Valentim CL, Cioli D, Chevalier FD, Cao X, Taylor AB, Holloway SP, Pica-Mattoccia L,
819 Guidi A, Basso A, Tsai IJ, et al: **Genetic and molecular basis of drug resistance and**
820 **species-specific drug action in schistosome parasites.** *Science* 2013, **342:**1385-1389.
821 14. Wang B, Collins JJ, 3rd, Newmark PA: **Functional genomic characterization of**
822 **neoblast-like stem cells in larval Schistosoma mansoni.** *Elife* 2013, **2:**e00768.
823 15. Collins JJ, 3rd, Wang B, Lambrus BG, Tharp ME, Iyer H, Newmark PA: **Adult somatic**
824 **stem cells in the human parasite Schistosoma mansoni.** *Nature* 2013, **494:**476-479.
825 16. Hagen J, Young ND, Every AL, Pagel CN, Schnoeller C, Scheerlinck JP, Gasser RB,
826 Kalinna BH: **Omega-1 knockdown in Schistosoma mansoni eggs by lentivirus**
827 **transduction reduces granuloma size in vivo.** *Nat Commun* 2014, **5:**5375.

828 17. Hoffmann KF, Brindley PJ, Berriman M: **Medicine. Halting harmful helminths.**
829 *Science* 2014, **346:**168-169.
830 18. Pearce EJ, MacDonald AS: **The immunobiology of schistosomiasis.** *Nat Rev Immunol*
831 2002, **2:**499-511.
832 19. Steinfelder S, Andersen JF, Cannons JL, Feng CG, Joshi M, Dwyer D, Caspar P,
833 Schwartzberg PL, Sher A, Jankovic D: **The major component in schistosome eggs**
834 **responsible for conditioning dendritic cells for Th2 polarization is a T2 ribonuclease**
835 **(omega-1).** *J Exp Med* 2009, **206:**1681-1690.
836 20. Everts B, Perona-Wright G, Smits HH, Hokke CH, van der Ham AJ, Fitzsimmons CM,
837 Doenhoff MJ, van der Bosch J, Mohrs K, Haas H, et al: **Omega-1, a glycoprotein**
838 **secreted by Schistosoma mansoni eggs, drives Th2 responses.** *J Exp Med* 2009,
839 **206:**1673-1680.
840 21. Pearce EJ, C MK, Sun J, J JT, McKee AS, Cervi L: **Th2 response polarization during**
841 **infection with the helminth parasite Schistosoma mansoni.** *Immunol Rev* 2004,
842 **201:**117-126.
843 22. Everts B, Hussaarts L, Driessen NN, Meevissen MH, Schramm G, van der Ham AJ, van
844 der Hoeven B, Scholzen T, Burgdorf S, Mohrs M, et al: **Schistosome-derived omega-1**
845 **drives Th2 polarization by suppressing protein synthesis following internalization**
846 **by the mannose receptor.** *J Exp Med* 2012, **209:**1753-1767, S1751.
847 23. Dunne DW, Jones FM, Doenhoff MJ: **The purification, characterization, serological**
848 **activity and hepatotoxic properties of two cationic glycoproteins (alpha 1 and omega**
849 **1) from Schistosoma mansoni eggs.** *Parasitology* 1991, **103 Pt 2:**225-236.
850 24. Curwen RS, Ashton PD, Johnston DA, Wilson RA: **The Schistosoma mansoni soluble**
851 **proteome: a comparison across four life-cycle stages.** *Mol Biochem Parasitol* 2004,
852 **138:**57-66.
853 25. Ashton PD, Harrop R, Shah B, Wilson RA: **The schistosome egg: development and**
854 **secretions.** *Parasitology* 2001, **122:**329-338.
855 26. Cass CL, Johnson JR, Califf LL, Xu T, Hernandez HJ, Stadecker MJ, Yates JR, 3rd,
856 Williams DL: **Proteomic analysis of Schistosoma mansoni egg secretions.** *Mol*
857 *Biochem Parasitol* 2007, **155:**84-93.
858 27. Mathieson W, Wilson RA: **A comparative proteomic study of the undeveloped and**
859 **developed Schistosoma mansoni egg and its contents: the miracidium, hatch fluid**
860 **and secretions.** *Int J Parasitol* 2010, **40:**617-628.
861 28. Wilbers RH, Westerhof LB, van Noort K, Obieglo K, Driessen NN, Everts B, Gringhuis
862 SI, Schramm G, Goverse A, Smant G, et al: **Production and glyco-engineering of**
863 **immunomodulatory helminth glycoproteins in plants.** *Sci Rep* 2017, **7:**45910.
864 29. Fitzsimmons CM, Schramm G, Jones FM, Chalmers IW, Hoffmann KF, Grevelding CG,
865 Wuhrer M, Hokke CH, Haas H, Doenhoff MJ, Dunne DW: **Molecular characterization**
866 **of omega-1: a hepatotoxic ribonuclease from Schistosoma mansoni eggs.** *Mol*
867 *Biochem Parasitol* 2005, **144:**123-127.
868 30. Ferguson BJ, Newland SA, Gibbs SE, Tourlomousis P, Fernandes dos Santos P, Patel
869 MN, Hall SW, Walczak H, Schramm G, Haas H, et al: **The Schistosoma mansoni T2**
870 **ribonuclease omega-1 modulates inflammasome-dependent IL-1beta secretion in**
871 **macrophages.** *Int J Parasitol* 2015, **45:**809-813.
872 31. Wynn TA, Thompson RW, Cheever AW, Mentink-Kane MM: **Immunopathogenesis of**
873 **schistosomiasis.** *Immunol Rev* 2004, **201:**156-167.

874 32. Jinek M, Chylinski K, Fonfara I, Hauer M, Doudna JA, Charpentier E: **A programmable**
875 **dual-RNA-guided DNA endonuclease in adaptive bacterial immunity.** *Science* 2012,
876 **337:**816-821.
877 33. Hsu PD, Lander ES, Zhang F: **Development and applications of CRISPR-Cas9 for**
878 **genome engineering.** *Cell* 2014, **157:**1262-1278.
879 34. Murare HM, Dunne DW, Bain J, Doenhoff MJ: **Schistosoma mansoni: control of**
880 **hepatotoxicity and egg excretion by immune serum in infected immunosuppressed**
881 **mice is schistosome species-specific, but not S. mansoni strain-specific.** *Exp Parasitol*
882 1992, **75:**329-339.
883 35. Lee AH, Symington LS, Fidock DA: **DNA repair mechanisms and their biological**
884 **roles in the malaria parasite Plasmodium falciparum.** *Microbiol Mol Biol Rev* 2014,
885 **78:**469-486.
886 36. Deriano L, Roth DB: **Modernizing the nonhomologous end-joining repertoire:**
887 **alternative and classical NHEJ share the stage.** *Annu Rev Genet* 2013, **47:**433-455.
888 37. International Helminth Genomes Consortium; Coghlan A, Mireva, M., Berriman, M.:
889 **Comparative genomics of the major parasitic worms.** *bioRxiv* 2017,
890 https://www.biorxiv.org/content/early/2017/12/20/236539
891 38. Lok JB, Shao H, Massey HC, Li X: **Transgenesis in Strongyloides and related**
892 **parasitic nematodes: historical perspectives, current functional genomic**
893 **applications and progress towards gene disruption and editing.** *Parasitology* 2017,
894 **144:**327-342.
895 39. Gang SS, Castelletto ML, Bryant AS, Yang E, Mancuso N, Lopez JB, Pellegrini M,
896 Hallem EA: **Targeted mutagenesis in a human-parasitic nematode.** *PLoS Pathog*
897 2017, **13:**e1006675.
898 40. Chen F, Pruett-Miller SM, Davis GD: **Gene editing using ssODNs with engineered**
899 **endonucleases.** *Methods Mol Biol* 2015, **1239:**251-265.
900 41. Suttiprapa S, Rinaldi G, Tsai IJ, Mann VH, Dubrovsky L, Yan HB, Holroyd N, Huckvale
901 T, Durrant C, Protasio AV, et al: **HIV-1 Integrates Widely throughout the Genome of**
902 **the Human Blood Fluke Schistosoma mansoni.** *PLoS Pathog* 2016, **12:**e1005931.
903 42. Duvoisin R, Ayuk MA, Rinaldi G, Suttiprapa S, Mann VH, Lee CM, Harris N, Brindley
904 PJ: **Human U6 promoter drives stronger shRNA activity than its schistosome**
905 **orthologue in Schistosoma mansoni and human fibrosarcoma cells.** *Transgenic Res*
906 2012, **21:**511-521.
907 43. Shah AN, Davey CF, Whitebirch AC, Miller AC, Moens CB: **Rapid reverse genetic**
908 **screening using CRISPR in zebrafish.** *Nat Methods* 2015, **12:**535-540.
909 44. Yu C, Zhang Y, Yao S, Wei Y: **A PCR based protocol for detecting indel mutations**
910 **induced by TALENs and CRISPR/Cas9 in zebrafish.** *PLoS One* 2014, **9:**e98282.
911 45. Pinello L, Canver MC, Hoban MD, Orkin SH, Kohn DB, Bauer DE, Yuan GC:
912 **Analyzing CRISPR genome-editing experiments with CRISPResso.** *Nat Biotechnol*
913 2016, **34:**695-697.
914 46. Suttiprapa S, Rinaldi G, Brindley PJ: **Prototypic chromatin insulator cHS4 protects**
915 **retroviral transgene from silencing in Schistosoma mansoni.** *Transgenic Res* 2012,
916 **21:**555-566.
917 47. Ke XD, Shen S, Song LJ, Yu CX, Kikuchi M, Hirayama K, Gao H, Wang J, Yin X, Yao
918 Y, et al: **Characterization of Schistosoma japonicum CP1412 protein as a novel**

919 **member of the ribonuclease T2 molecule family with immune regulatory function.**
920 *Parasit Vectors* 2017, **10:**89.
921 48. Zaccone P, Burton OT, Gibbs SE, Miller N, Jones FM, Schramm G, Haas H, Doenhoff
922 MJ, Dunne DW, Cooke A: **The S. mansoni glycoprotein omega-1 induces Foxp3**
923 **expression in NOD mouse CD4(+) T cells.** *Eur J Immunol* 2011, **41:**2709-2718.
924 49. Ritter M, Gross O, Kays S, Ruland J, Nimmerjahn F, Saijo S, Tschopp J, Layland LE,
925 Prazeres da Costa C: **Schistosoma mansoni triggers Dectin-2, which activates the**
926 **Nlrp3 inflammasome and alters adaptive immune responses.** *Proc Natl Acad Sci U S*
927 *A* 2010, **107:**20459-20464.
928 50. Qin Z: **The use of THP-1 cells as a model for mimicking the function and regulation**
929 **of monocytes and macrophages in the vasculature.** *Atherosclerosis* 2012, **221:**2-11.
930 51. Fuentes L, Hernandez M, Fernandez-Aviles FJ, Crespo MS, Nieto ML: **Cooperation**
931 **between secretory phospholipase A2 and TNF-receptor superfamily signaling:**
932 **implications for the inflammatory response in atherogenesis.** *Circ Res* 2002, **91:**681-
933 688.
934 52. Doenhoff MJ, Hassounah O, Murare H, Bain J, Lucas S: **The schistosome egg**
935 **granuloma: immunopathology in the cause of host protection or parasite survival?**
936 *Trans R Soc Trop Med Hyg* 1986, **80:**503-514.
937 53. Boros DL, Warren KS: **Delayed hypersensitivity-type granuloma formation and**
938 **dermal reaction induced and elicited by a soluble factor isolated from Schistosoma**
939 **mansoni eggs.** *J Exp Med* 1970, **132:**488-507.
940 54. Eltoum IA, Wynn TA, Poindexter RW, Finkelman FD, Lewis FA, Sher A, Cheever AW:
941 **Suppressive effect of interleukin-4 neutralization differs for granulomas around**
942 **Schistosoma mansoni eggs injected into mice compared with those around eggs laid**
943 **in infected mice.** *Infect Immun* 1995, **63:**2532-2536.
944 55. Wynn TA, Eltoum I, Cheever AW, Lewis FA, Gause WC, Sher A: **Analysis of cytokine**
945 **mRNA expression during primary granuloma formation induced by eggs of**
946 **Schistosoma mansoni.** *J Immunol* 1993, **151:**1430-1440.
947 56. Lieber MR: **The mechanism of double-strand DNA break repair by the**
948 **nonhomologous DNA end-joining pathway.** *Annu Rev Biochem* 2010, **79:**181-211.
949 57. Paquet D, Kwart D, Chen A, Sproul A, Jacob S, Teo S, Olsen KM, Gregg A, Noggle S,
950 Tessier-Lavigne M: **Efficient introduction of specific homozygous and heterozygous**
951 **mutations using CRISPR/Cas9.** *Nature* 2016, **533:**125-129.
952 58. Zhang WW, Matlashewski G: **CRISPR-Cas9-Mediated Genome Editing in**
953 **Leishmania donovani.** *MBio* 2015, **6:**e00861.
954 59. Yoshimi K, Kunihiro Y, Kaneko T, Nagahora H, Voigt B, Mashimo T: **ssODN-mediated**
955 **knock-in with CRISPR-Cas for large genomic regions in zygotes.** *Nature*
956 *communications* 2016, **7:**10431.
957 60. Jurberg AD, Goncalves T, Costa TA, de Mattos AC, Pascarelli BM, de Manso PP,
958 Ribeiro-Alves M, Pelajo-Machado M, Peralta JM, Coelho PM, Lenzi HL: **The**
959 **embryonic development of Schistosoma mansoni eggs: proposal for a new staging**
960 **system.** *Dev Genes Evol* 2009, **219:**219-234.
961 61. Neill PJ, Smith JH, Doughty BL, Kemp M: **The ultrastructure of the Schistosoma**
962 **mansoni egg.** *Am J Trop Med Hyg* 1988, **39:**52-65.
963 62. Mann VH, Suttiprapa S, Rinaldi G, Brindley PJ: **Establishing transgenic schistosomes.**
964 *PLoS Negl Trop Dis* 2011, **5:**e1230.

965 63. Kosicki M, Rajan SS, Lorenzetti FC, Wandall HH, Narimatsu Y, Metzakopian E, Bennett
966 EP: **Dynamics of Indel Profiles Induced by Various CRISPR/Cas9 Delivery**
967 **Methods.** *Prog Mol Biol Transl Sci* 2017, **152:**49-67.
968 64. Holmgaard A, Askou AL, Benckendorff JNE, Thomsen EA, Cai Y, Bek T, Mikkelsen
969 JG, Corydon TJ: **In Vivo Knockout of the Vegfa Gene by Lentiviral Delivery of**
970 **CRISPR/Cas9 in Mouse Retinal Pigment Epithelium Cells.** *Mol Ther Nucleic Acids*
971 2017, **9:**89-99.
972 65. Yu Z, Chen Q, Chen W, Zhang X, Mei F, Zhang P, Zhao M, Wang X, Shi N, Jackson S,
973 Hong Y: **Multigene editing via CRISPR/Cas9 guided by a single-sgRNA seed in**
974 **Arabidopsis.** *J Integr Plant Biol* 2018, **60:**376-381.
975 66. Luo JJ, Bian WP, Liu Y, Huang HY, Yin Q, Yang XJ, Pei DS: **CRISPR/Cas9-based**
976 **genome engineering of zebrafish using a seamless integration strategy.** *FASEB J*
977 2018**:**fj201800077RR.
978 67. Shalem O, Sanjana NE, Zhang F: **High-throughput functional genomics using**
979 **CRISPR-Cas9.** *Nat Rev Genet* 2015, **16:**299-311.
980 68. Kines KJ, Rinaldi G, Okatcha TI, Morales ME, Mann VH, Tort JF, Brindley PJ:
981 **Electroporation facilitates introduction of reporter transgenes and virions into**
982 **schistosome eggs.** *PLoS Negl Trop Dis* 2010, **4:**e593.
983 69. Heyer WD, Ehmsen KT, Liu J: **Regulation of homologous recombination in**
984 **eukaryotes.** *Annu Rev Genet* 2010, **44:**113-139.
985 70. Schramm G, Hamilton JV, Balog CI, Wuhrer M, Gronow A, Beckmann S, Wippersteg V,
986 Grevelding CG, Goldmann T, Weber E, et al: **Molecular characterisation of kappa-5, a**
987 **major antigenic glycoprotein from Schistosoma mansoni eggs.** *Mol Biochem Parasitol*
988 2009, **166:**4-14.
989 71. Brogna S, Wen J: **Nonsense-mediated mRNA decay (NMD) mechanisms.** *Nat Struct*
990 *Mol Biol* 2009, **16:**107-113.
991 72. Pankowicz FP, Jarrett KE, Lagor WR, Bissig KD: **CRISPR/Cas9: at the cutting edge of**
992 **hepatology.** *Gut* 2017, **66:**1329-1340.
993 73. Kaisar MMM, Ritter M, Del Fresno C, Jonasdottir HS, van der Ham AJ, Pelgrom LR,
994 Schramm G, Layland LE, Sancho D, Prazeres da Costa C, et al: **Dectin-1/2-induced**
995 **autocrine PGE2 signaling licenses dendritic cells to prime Th2 responses.** *PLoS Biol*
996 2018, **16:**e2005504.
997 74. Dalton JP, Day SR, Drew AC, Brindley PJ: **A method for the isolation of schistosome**
998 **eggs and miracidia free of contaminating host tissues.** *Parasitology* 1997, **115 (Pt**
999 **1):**29-32.
1000 75. Mann VH, Morales ME, Rinaldi G, Brindley PJ: **Culture for genetic manipulation of**
1001 **developmental stages of Schistosoma mansoni.** *Parasitology* 2010, **137:**451-462.
1002 76. Mann VH, Suttiprapa S, Skinner DE, Brindley PJ, Rinaldi G: **Pseudotyped murine**
1003 **leukemia virus for schistosome transgenesis: approaches, methods and perspectives.**
1004 *Transgenic Res* 2014, **23:**539-556.
1005 77. Cardoso LS, Araujo MI, Goes AM, Pacifico LG, Oliveira RR, Oliveira SC: **Polymyxin B**
1006 **as inhibitor of LPS contamination of Schistosoma mansoni recombinant proteins in**
1007 **human cytokine analysis.** *Microb Cell Fact* 2007, **6:**1.
1008 78. Bradford MM: **A rapid and sensitive method for the quantitation of microgram**
1009 **quantities of protein utilizing the principle of protein-dye binding.** *Anal Biochem*
1010 1976, **72:**248-254.

1011 79. Oliveros JC, Franch M, Tabas-Madrid D, San-Leon D, Montoliu L, Cubas P, Pazos F:
1012 **Breaking-Cas-interactive design of guide RNAs for CRISPR-Cas experiments for**
1013 **ENSEMBL genomes.** *Nucleic Acids Res* 2016, **44:**W267-271.
1014 80. Minskaia E, Nicholson J, Ryan MD: **Optimisation of the foot-and-mouth disease virus**
1015 **2A co-expression system for biomedical applications.** *BMC Biotechnol* 2013, **13:**67.
1016 81. Lok JB, Shao H, Massey HC, Li X: **Transgenesis in Strongyloides and related**
1017 **parasitic nematodes: historical perspectives, current functional genomic**
1018 **applications and progress towards gene disruption and editing.** *Parasitology* 2016**:**1-
1019 16.
1020 82. Marozsan AJ, Fraundorf E, Abraha A, Baird H, Moore D, Troyer R, Nankja I, Arts EJ:
1021 **Relationships between infectious titer, capsid protein levels, and reverse**
1022 **transcriptase activities of diverse human immunodeficiency virus type 1 isolates.** *J*
1023 *Virol* 2004, **78:**11130-11141.
1024 83. Martin M: **Cutadapt removes adapter sequences from high-throughput sequencing**
1025 **reads.** *EMBnetjournal North America* 2011,
1026 http://journal.embnet.org/index.php/embnetjournal/article/view/200/458.
1027 84. Canver MC, Haeussler M, Bauer DE, Orkin SH, Sanjana NE, Shalem O, Yuan GC,
1028 Zhang F, Concordet JP, Pinello L: **Integrated design, execution, and analysis of**
1029 **arrayed and pooled CRISPR genome-editing experiments.** *Nat Protoc* 2018, **13:**946-
1030 986.
1031 85. Pearson WR, Lipman DJ: **Improved tools for biological sequence comparison.** *Proc*
1032 *Natl Acad Sci U S A* 1988, **85:**2444-2448.
1033 86. Ginzinger DG: **Gene quantification using real-time quantitative PCR: an emerging**
1034 **technology hits the mainstream.** *Exp Hematol* 2002, **30:**503-512.
1035 87. Livak KJ, Schmittgen TD: **Analysis of relative gene expression data using real-time**
1036 **quantitative PCR and the 2(-Delta Delta C(T)) Method.** *Methods* 2001, **25:**402-408.
1037 88. Cheever AW, Finkelman FD, Caspar P, Heiny S, Macedonia JG, Sher A: **Treatment**
1038 **with anti-IL-2 antibodies reduces hepatic pathology and eosinophilia in Schistosoma**
1039 **mansoni-infected mice while selectively inhibiting T cell IL-5 production.** *J Immunol*
1040 1992, **148:**3244-3248.
1041 89. Genin M, Clement F, Fattaccioli A, Raes M, Michiels C: **M1 and M2 macrophages**
1042 **derived from THP-1 cells differentially modulate the response of cancer cells to**
1043 **etoposide.** *BMC Cancer* 2015, **15:**577.
1044 90. Schmid MC, Varner JA: **Myeloid cells in the tumor microenvironment: modulation of**
1045 **tumor angiogenesis and tumor inflammation.** *J Oncol* 2010, **2010:**201026.
1046 91. Chomczynski P: **A reagent for the single-step simultaneous isolation of RNA, DNA**
1047 **and proteins from cell and tissue samples.** *Biotechniques* 1993, **15:**532-534, 536-537.
1048 92. Crooks GE, Hon G, Chandonia JM, Brenner SE: **WebLogo: a sequence logo generator.**
1049 *Genome Res* 2004, **14:**1188-1190.
1050 93. Gieseck RL, 3rd, Wilson MS, Wynn TA: **Type 2 immunity in tissue repair and**
1051 **fibrosis.** *Nat Rev Immunol* 2018, **18:**62-76.
1052 94. Wynn TA: **Type 2 cytokines: mechanisms and therapeutic strategies.** *Nat Rev*
1053 *Immunol* 2015, **15:**271-282.
1054 95. Larkin MA, Blackshields G, Brown NP, Chenna R, McGettigan PA, McWilliam H,
1055 Valentin F, Wallace IM, Wilm A, Lopez R, et al: **Clustal W and Clustal X version 2.0.**
1056 *Bioinformatics* 2007, **23:**2947-2948.

1057

Figure 1

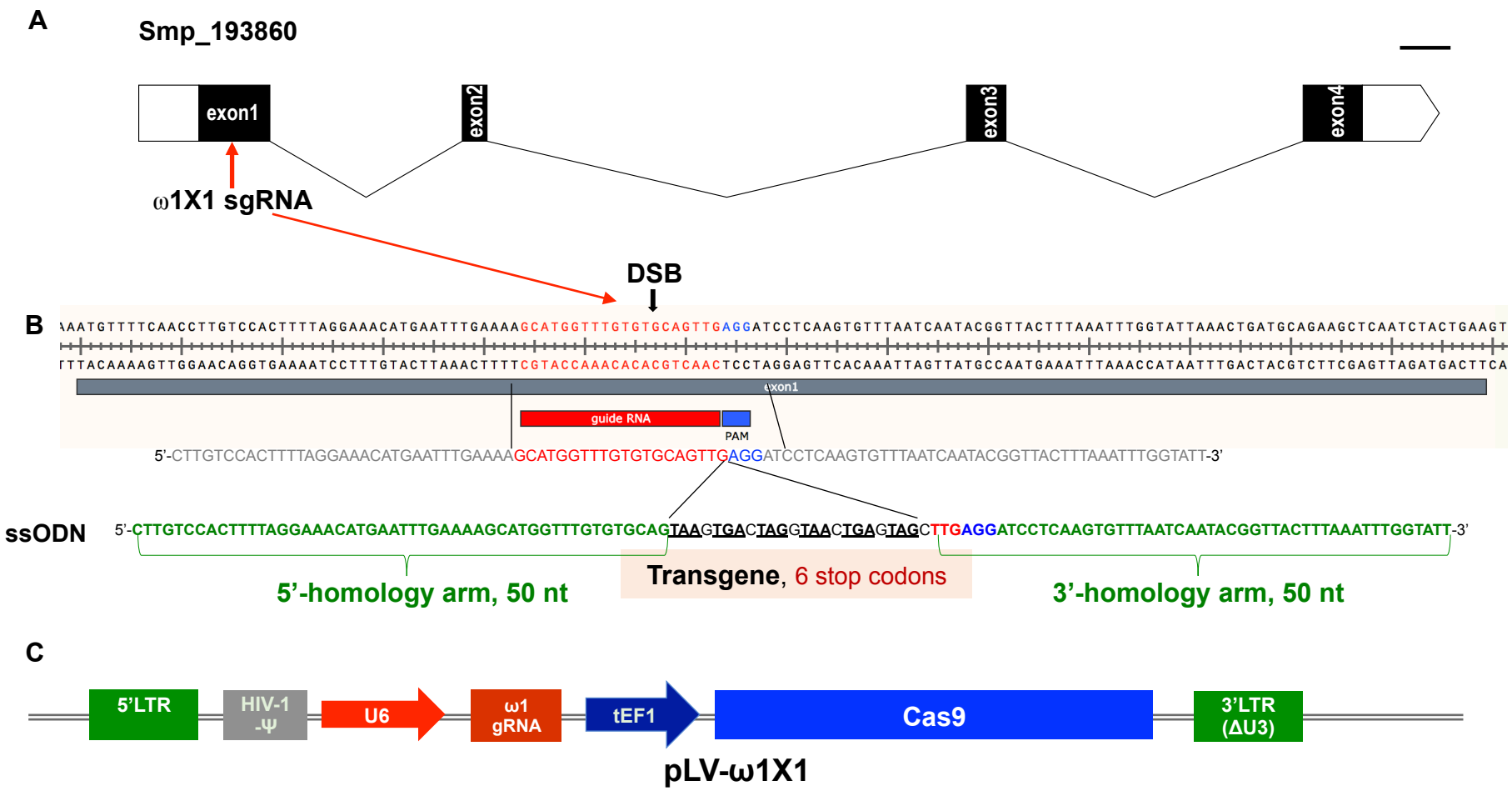
A
Smp_193860
exon1
exon2
exon3
exon4
ω1X1 sgRNA
DSB
B
exon1
guide RNA
PAM
5'-CTTGTCCACTTTTAGGAAACATGAATTTGAAAAGCATGGTTTGTGTGCAGTTGAGGATCCTCAAGTGTTTAATCAATACGGTTACTTTAAATTTGGTATT-3'
ssODN
5'-CTTGTCCACTTTTAGGAAACATGAATTTGAAAAGCATGGTTTGTGTGCAGTAAGTGACTAGGTAACTGAGTAGCTTGAGGATCCTCAAGTGTTTAATCAATACGGTTACTTTAAATTTGGTATT-3'
5'-homology arm, 50 nt
Transgene, 6 stop codons
3'-homology arm, 50 nt
C
5'LTR
HIV-1 -Ψ
U6
ω1 gRNA
tEF1
Cas9
3'LTR (ΔU3)
pLV-ω1X1

Figure 2

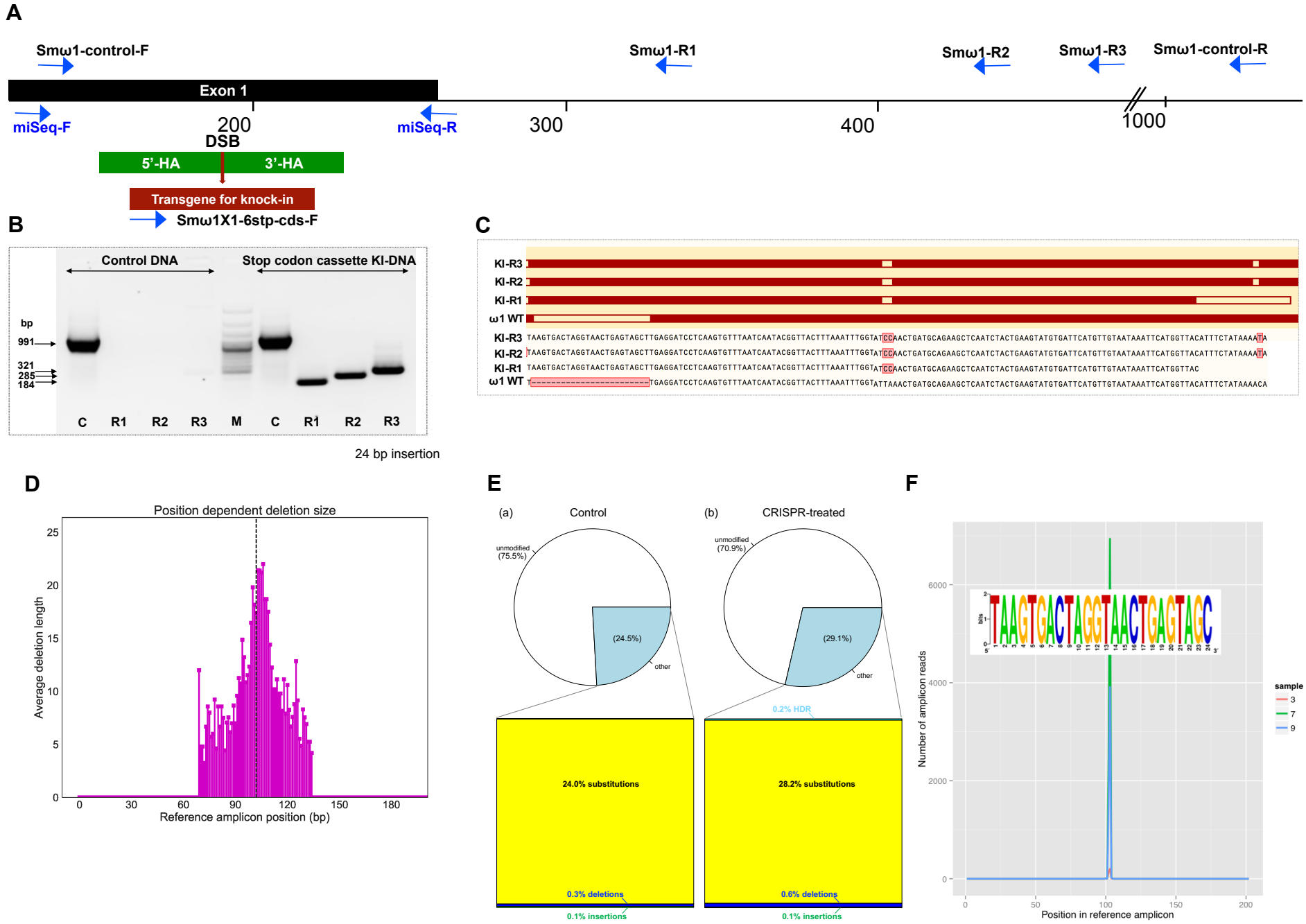
A
Smω1-control-F
Smω1-R1
Smω1-R2
Smω1-R3
Smω1-control-R
Exon 1
miSeq-F
miSeq-R
200
300
400
1000
DSB
5'-HA
3'-HA
Transgene for knock-in
Smω1X1-6stp-cds-F
B
Control DNA
Stop codon cassette KI-DNA
bp
991
321
285
184
C
R1
R2
R3
M
C
R1
R2
R3
24 bp insertion
C
KI-R3
KI-R2
KI-R1
ω1 WT
D
Position dependent deletion size
Average deletion length
Reference amplicon position (bp)
E
(a)
Control
(b)
CRISPR-treated
unmodified (75.5%)
(24.5%)
other
unmodified (70.9%)
(29.1%)
other
0.2% HDR
24.0% substitutions
28.2% substitutions
0.3% deletions
0.6% deletions
0.1% insertions
0.1% insertions
F
Number of amplicon reads
Position in reference amplicon
sample
3
7
9

Figure 3

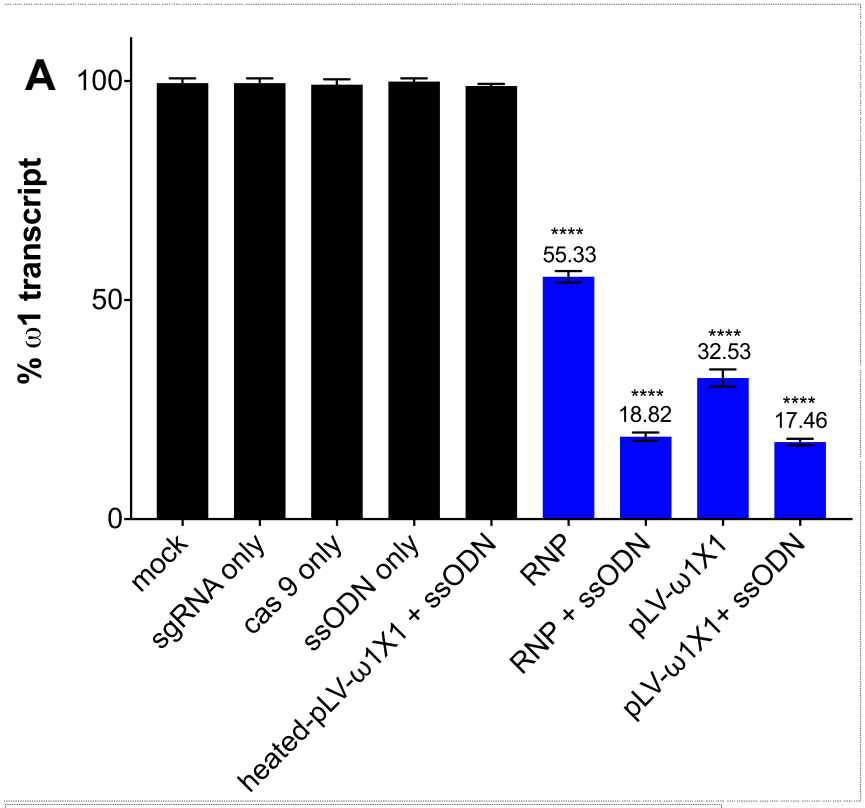
A
% ω1 transcript
100
50
0
****
55.33
****
18.82
****
32.53
****
17.46
mock
sgRNA only
cas 9 only
ssODN only
heated-pLV-ω1X1 + ssODN
RNP
RNP + ssODN
pLV-ω1X1
pLV-ω1X1+ ssODN

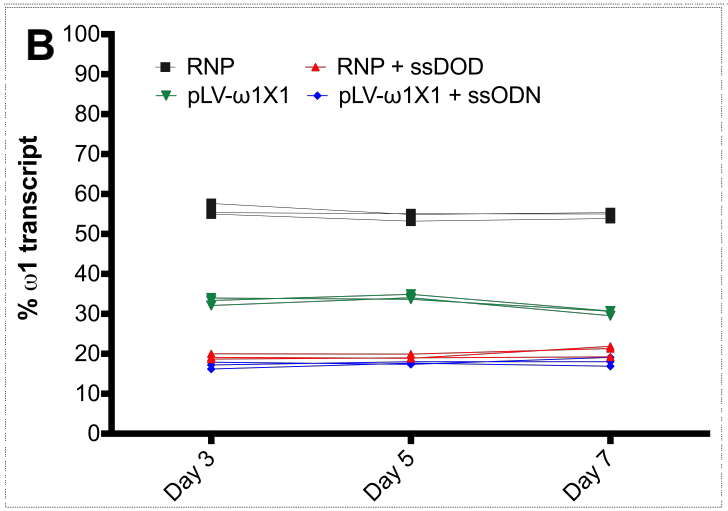
B
% ω1 transcript
RNP
RNP + ssDOD
pLV-ω1X1
pLV-ω1X1 + ssODN
Day 3
Day 5
Day 7

C
1
2
3
4
5
6
7
8
9
10
11
12

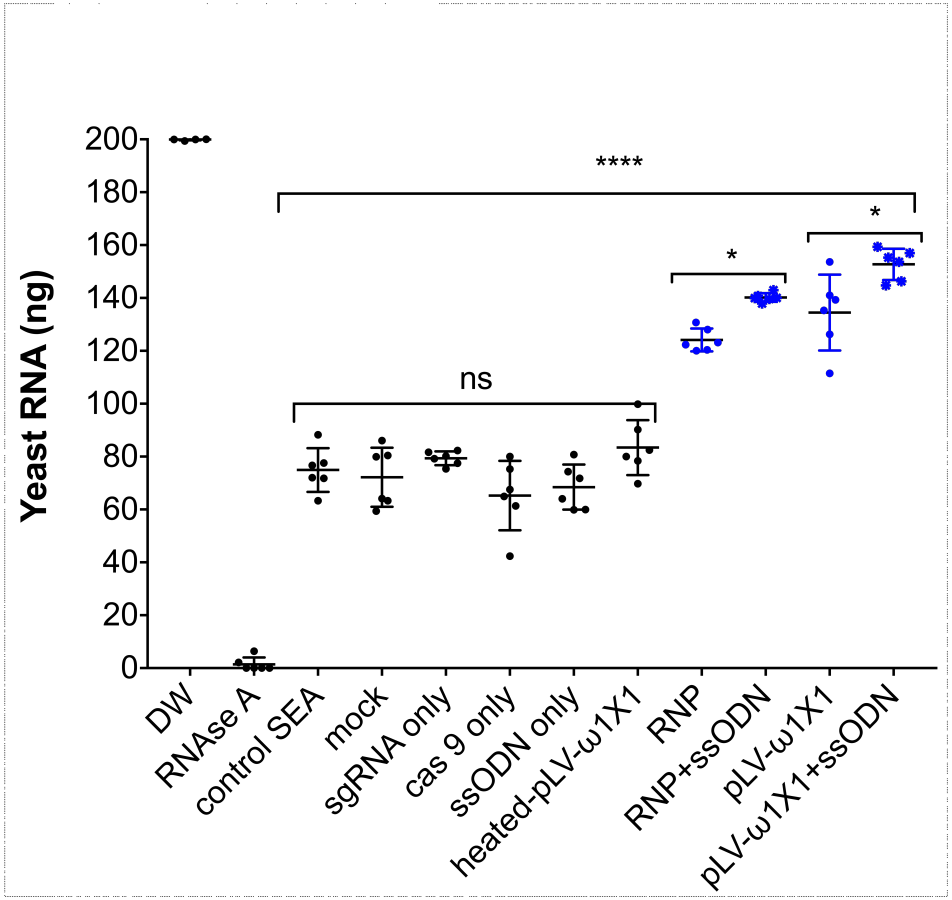
D
Yeast RNA (ng)
****
*
*
ns
DW
RNAse A
control SEA
mock
sgRNA only
cas 9 only
ssODN only
heated-pLV-ω1X1
RNP
RNP+ssODN
pLV-ω1X1
pLV-ω1X1+ssODN

Figure 4

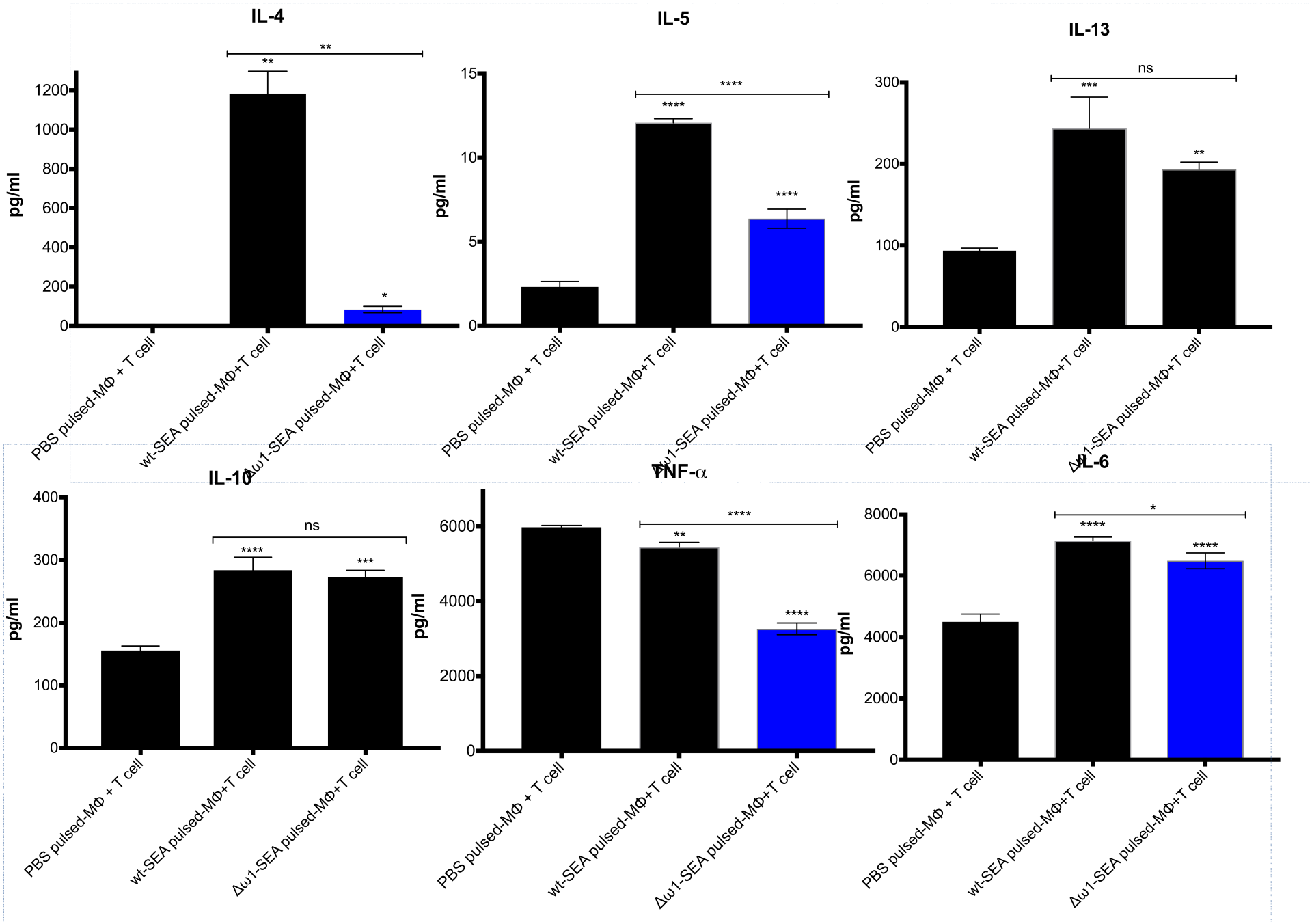
IL-4
IL-5
IL-13
IL-10
TNF-α
IL-6
pg/ml
PBS pulsed-Mφ + T cell
wt-SEA pulsed-Mφ+T cell
Δω1-SEA pulsed-Mφ+T cell
ns

Figure 5

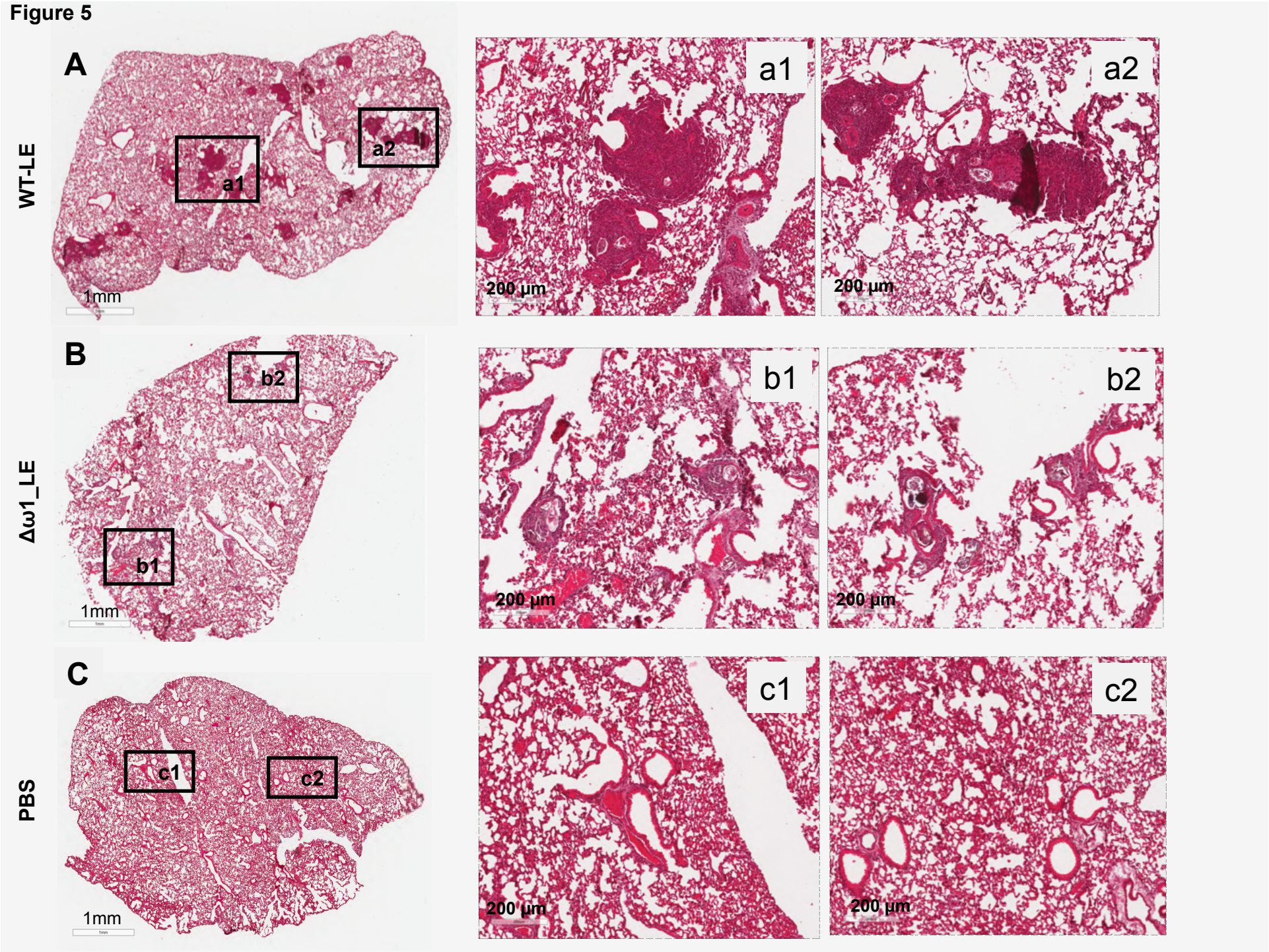
A
WT-LE
a1
a2
1mm
200 µm
200 µm
B
Δω1_LE
b1
b2
1mm
200 µm
200 µm
C
PBS
c1
c2
1mm
200 µm
200 µm
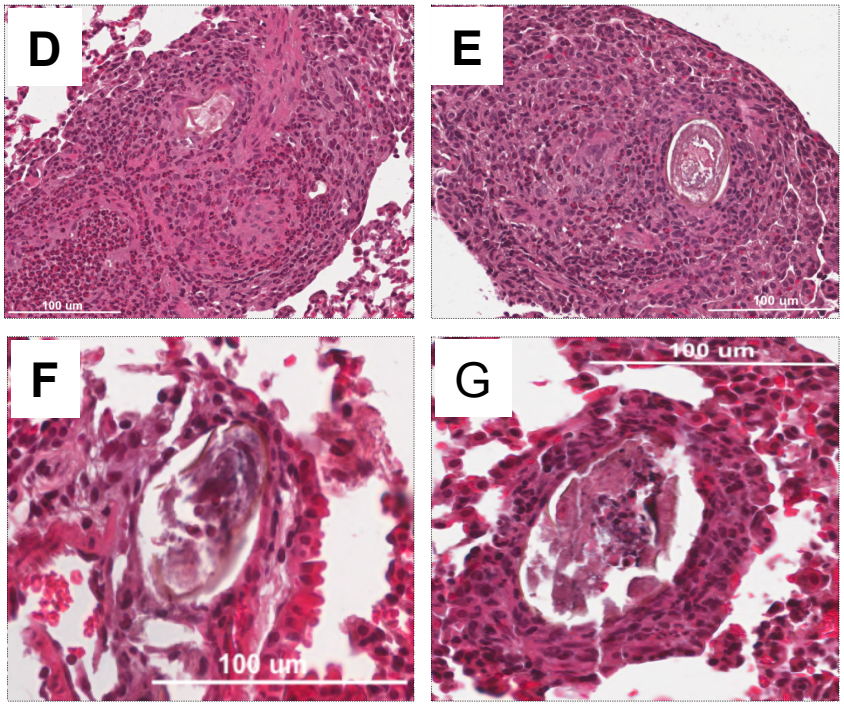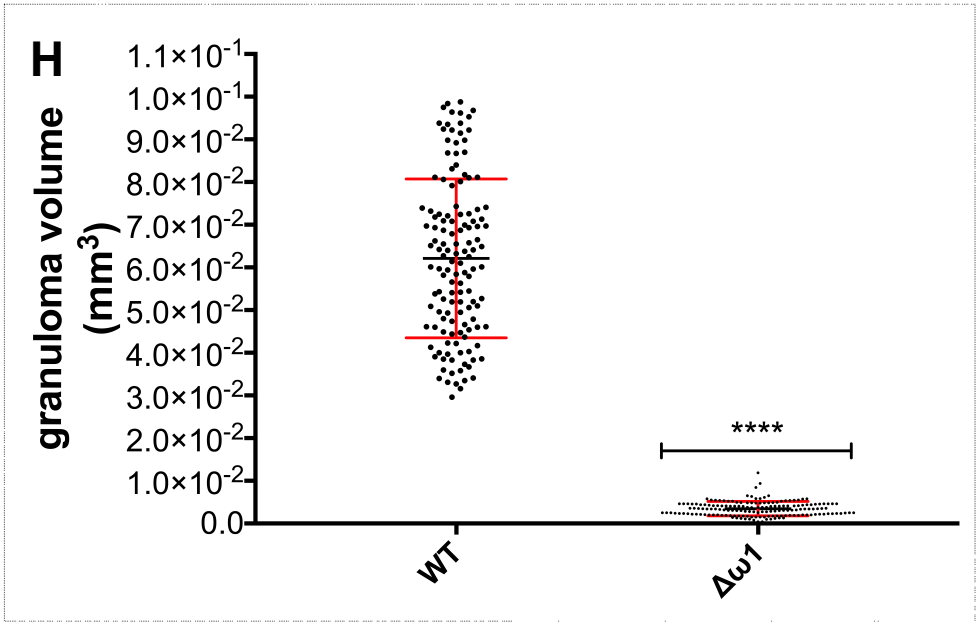
Figure 5 (cont.)